Post-print of: Wang, Rong et al. “Global forest carbon uptake due to nitrogen and phosphorus deposition from 1850 to 2100” in *Global Change Biology* (2017). DOI available at: ***https://doi.org/10.1111/gcb.13766***

Global forest carbon uptake due to nitrogen and phosphorus deposition from 1850 to 2100

Rong Wang[1,2,3], Daniel Goll[1,2], Yves Balkanski[1,2], Didier Hauglustaine[1,2], Olivier Boucher[4], Philippe Ciais[1,2], Ivan Janssens[5], Josep Penuelas[6,7], Bertrand Guenet[1,2], Jordi Sardans[6,7], Laurent Bopp[1,2], Nicolas Vuichard[1], Feng Zhou[2], Bengang Li[2], Shilong Piao[2], Shushi Peng[2], Ye Huang[1], Shu Tao[2]

[1]Laboratoire des Sciences du Climat et de l’Environnement, CEA CNRS UVSQ, 91190 Gif-sur-Yvette, France [2]Sino-French Institute for Earth System Science, College of Urban and Environmental Sciences, Peking University, 100871 Beijing, China [3]Department of Global Ecology, Carnegie Institution for Science, Stanford, 94305 California, USA [4]Laboratoire de Météorologie Dynamique, IPSL/CNRS, Université Pierre et Marie Curie, 75252 Paris, France [5]Department of Biology, University of Antwerp, Universiteitsplein 1, B-2610 Wilrijk, Belgium [6]CSIC, Global Ecology Unit CREAF-CSIC-UAB, Bellaterra, 08193 Catalonia, Spain [7]CREAF, Cerdanyola del Vallès, 08193 Catalonia, Spain

Correspondence to: Rong Wang (rong.wang@lsce.ipsl.fr)

Abstract:

Spatial patterns and temporal trend of nitrogen (N) and phosphorus (P) deposition are important for quantifying their impact on forest carbon (C) uptake. In a first step, we modeled historical and future change in the global distributions of the atmospheric deposition of N and P from the dry and wet deposition of aerosols and gases containing N and P. Future projections were compared between two scenarios with contrasting aerosol emissions. Modeled fields of N and P deposition and P concentration were evaluated using globally distributed *in situ* measurements. N deposition peaked around 1990 in European forests and around 2010 in East Asian forests, and both increased 7-fold relative to 1850. P deposition peaked around 2010 in South Asian forests and increased 3.5-fold relative to 1850. In a second step, we estimated the change in C storage in forests due to the fertilization by deposited N and P ($\Delta C_{v\ dep}$), based on the retention of deposited nutrients, their allocation within plants, and C:N and C:P stoichiometry. $\Delta C_{v\ dep}$ for 1997-2013 was estimated to be 0.27 ± 0.13 Pg C yr^{-1} from N and 0.054 ± 0.10 Pg C yr^{-1} from P, contributing 9% and 2% of the terrestrial C sink, respectively. Sensitivity tests show that uncertainty of $\Delta C_{v\ dep}$ was larger from P than from N, mainly due to uncertainty in the fraction of deposited P that is fixed by soil. $\Delta C_{P\ dep}$ was exceeded by $\Delta C_{N\ dep}$ over 1960-2007 in a large area of East Asian and West European forests due to a faster growth in N deposition than P. Our results suggest a significant contribution of anthropogenic P deposition to C storage, and additional sources of N are needed to support C storage by P in some Asian tropical forests where the deposition rate increased even faster for P than for N.

1. Introduction

The processes controlling the terrestrial carbon (C) sink are a major source of uncertainty in projections of the historical and future evolution of atmospheric CO_2 (Matthews, 2007; Ahlstrom *et al.*, 2012). Observations and models both suggest that terrestrial C sinks are limited by nitrogen (N) and phosphorus (P) with notable regional differences (Hungate *et al.*, 2004; Reich *et al.*, 2006; Elser *et al.*, 2007; Thornton *et al.*,2009, Norby *et al.*, 2010; Vitousek, *et al.*, 2010; Goll *et al.*, 2012, Penuelas *et al.*, 2013, Fernández-Martinez *et al.*, 2014; Wieder *et al.*, 2015). The majority of studies predict a large limitation of the C sink in the 21st century due to limited availabilities of N and P, but the extent of this limitation varies widely among studies. This effect of limitation implies that terrestrial C sinks are sensitive to the inputs of N and P from atmospheric deposition in the case of non-cultivated ecosystems. In particular, anthropogenic emissions of reactive N, including oxidized (*e.g.* NO_x) and reduced (*e.g.* NH_3) N have increased significantly in the past decades (Galloway *et al.*, 2004), causing notable change in N availability in northern temperate and boreal forests (Magnani *et al.*, 2007) and more recently in tropical forests (Hietz *et al.*, 2011). During 1982-2009, N deposition has contributed 9% to the observed greening of the Earth (Zhu *et al.*, 2016).

Atmospheric deposition increases the availability of N and P, and thus should increase or sustain the terrestrial C sink (Graham and Duce, 1979; Galloway *et al.*, 2004; Okin *et al.*, 2004; Mahowald, 2011). Nadelhoffer *et al.* (1999) estimated that N deposition accounts for a C sink of 0.25 Pg C yr^{-1} in 1990s based on ^{15}N tracer studies in nine forests and a prescribed N input of 5.1 Tg N yr^{-1} to the Earth's forests. For the same period, Liu and Greaver (2009) estimated a somewhat larger contribution of N deposition to the global terrestrial C sink of 0.35-0.58 Pg C yr^{-1} based on a meta-analysis of field observations. Thomas *et al.* (2010) attributed a C sink of 0.31 Pg C yr^{-1} to this factor in forests by comparing forest growth rates for different exposures of N deposition during the 1980s and 1990s based on data from the national forest inventory in the USA. Zaehle *et al.* (2010, 2014) estimated that N deposition resulted in a net terrestrial C sink of 0.2 Pg C yr^{-1} during 1996-2005 using an OCN process-based vegetation model. de Vries *et al.* (2014) estimated a contribution of comparable magnitude (0.2-0.5 Pg C yr^{-1}) from N deposition to the global land C sink using a stoichiometric approach. While the impact of atmospheric N deposition on terrestrial C sink has been assessed by several studies, the contribution of P deposition has not yet been quantified. This is because reconstruction of historical changes in P deposition are lacking.

Several studies have attempted to simulate the spatial distributions of N deposition (Holland *et al.*, 1997; Lamarque *et al.*, 2005, 2013; Dentener *et al.*, 2006; Phoenix *et al.*, 2006; Paulot *et al.*, 2013; Hauglustaine *et al.*, 2014) and P deposition (Mahowald *et al.*, 2008) under current and future conditions driven by emission inventories. These studies differ by their emission inventories, aerosol chemistry and horizontal resolutions of chemical transport models (CTM) (**Table S1**). However, the modeled N and P deposition rates are subject to high uncertainty, which remains unquantified. For example, the modeled wet deposition rates of nitrate (NO_3) and ammonium (NH_4) as means of 11 CTMs were underestimated by 40-140% compared to atmospheric station data depending on the region (Lamarque *et al.*, 2013). Hauglustaine *et al.* (2014) suggested that the underestimation in wet N deposition for Asia in their CTM is of 50-60% due to a

bias in the region's N emissions estimates and the model's coarse horizontal resolution. Earlier estimates of present day total P deposition (Mahowald *et al.*, 2008) were underestimated by almost one order of magnitude, likely due to an underestimation of the contribution of human activities to P emissions (Wang *et al.*, 2015a). Recent measurements in China underline the anthropogenic component of P deposition showing that the bulk deposition of P followed a power-law increase with decreasing distance of monitoring sites to the nearest cities (Du *et al.*, 2016). More measurements over a wide range of representative stations are necessary to confirm the regional contribution of combustion sources to P in the atmosphere. High-resolution data sets of modeled N and P deposition over forests supported by global measurements are critical for understanding the C sink that offsets the increase in fossil-fuel C emissions and the limitations of primary productivity by N and P. However, such data sets are not available due to uncertainties in the emission inventories of N and P and limited understanding of N chemistry in aerosols.

Elemental stoichiometry has been used to identify major constraints in the change in C storage by terrestrial ecosystems due to nutrients either available in soils or deposited from the atmosphere, based on assumptions about the allocation of nutrients and their elemental ratios (e.g., C:N or C:P) in ecosystemic C pools. This method assumes that N and P limitation of net primary productivity (NPP) is widespread across global biomes (Elser *et al.*, 2007). For example, Cleveland *et al.* (2013) used this method to show that external inputs of N and P through atmospheric deposition supports 3.8% and 16% of new NPP, but the uncertainty has not been considered. De Vries *et al.* (2014) used this method to infer that N deposition supports a global forest C sink of 0.28-0.45 Pg C yr^{-1} by assuming that 15% of deposited N is retained in forest biomass and 15% in soil in tropical forests, but the impact of P was not considered in this study.

Our study aims to fill these gaps by providing the first time-series of N & P deposition and the resulting C sink taking into account the major sources of uncertainty. To do so, we calculated the temporal evolutions of N and P deposition in a CTM prescribed by reconstructions of historical and future scenarios of anthropogenic emissions and evaluated the so derived N wet deposition, P total deposition and surface P concentrations in aerosols with in situ measurements. We built a modeling framework to estimate the C sequestration of global forests due to historical and future N and P deposition. We accounted for uncertainties in the stoichiometric and allocation parameters by employing a Monte Carlo method in a stoichiometric mass-balance approach, and identify key factors influencing the forest C sequestration.

2. Materials and methods

2.1. Atmospheric deposition of N and P for 1850-2100

The global aerosol chemistry climate model LMDZ-INCA couples the LMDz (Laboratoire de Météorologie Dynamique, version-4) General Circulation Model (Hourdin *et al.*, 2006) and the INCA (INteraction with Chemistry and Aerosols, version-4) aerosol module (Hauglustaine *et al.*, 2014). A full description of the model is provided in the **Supporting Information**. To run the model, emissions data included sea-salt and dust for P, primary biogenic aerosol particles for P, oceanic emissions for N (NH_3), vegetation emissions for N (NO), agricultural activities (including fertilizer use and livestock) for N, and fuel combustion for both N (NO_y and NH_x) and P. Regarding N-containing aerosols and gases,

LMDZ-INCA was run with a fully interactive atmospheric N cycle (Hauglustaine *et al.*, 2014) at a horizontal resolution of 1.27° latitude by 2.5° longitude with 39 vertical layers in the atmosphere to simulate the global dry and wet deposition of NO_y and NH_x for 1850, 1960, 1970, 1980, 1990, 1997-2013, 2030, 2050 and 2100. The same resolution is used for the transport and deposition of P aerosols in LMDZ-INCA with the emission data provided by Wang *et al.* (2015a), which are transported in three size bins for P emitted by combustion processes with a diagnostic mass median diameter (MMD) of 0.14, 2.5 and 10.0 μm, one size bin for P from primary biogenic aerosol particles (MMD=5.0 μm), one size bin for P from mineral dust (MMD=2.5 μm), and three size bins for P from marine sea-salt particles (Balkanski *et al.*, 2011). Meteorological fields from a reanalysis of the European Centre for Medium-Range Weather Forecasts (ECMWF) have been used in the present configuration to nudge the model transport and removal processes for 1980 and 1990 and for each year during the recent 1997-2013 period. Additional simulations were performed with emissions for 1850, 1960, 1970 and into the future all using meteorological fields for 2005.

The emissions prescribed to LMDZ-INCA were obtained from published data sets or emission inventories. We focused on generating coherent emission data sets for all species, and the methods are fully described in the **Supporting Information**. **Table S2** lists the emission data sets used in our study. In brief, global 0.5°×0.5° emissions of NO_x, NH_3, sulfur dioxide (SO_2), non-methane volatile organic compounds (NMVOCs), methane (CH_4), carbon monoxide (CO), organic carbon (OC) and black carbon (BC) for 2005, 2010 and 2030 were obtained from the ECLIPSE.GAINS.4a model (Klimont *et al.*, 2013). SO_2, CO, CH_4 and NMVOCs species should be treated consistently with N aerosols, because they influence N chemistry in the model (Hauglustaine *et al.*, 2014). The ECLIPSE.GAINS.4a emissions of all species were extended to other years of simulations using historical data from the ACCMIP and MACCity inventories (Lamarque *et al.*, 2010; Granier *et al.*, 2011) and future data from the RCP4.5 and RCP8.5 scenarios by Lamarque *et al.* (2011). In addition, natural emissions of NO and NH_3 from soil (Bouwman *et al.*, 1997; Lathière *et al.*, 2006) were assumed to be constant throughout the period; natural oceanic emissions of NH_3 were calculated in the INCA model following the formulations proposed by Paulot *et al.* (2015), with monthly 2°×2° fields of surface sea-water concentrations of NH_4, pH and salinity as simulated by the oceanic biogeochemical model PISCES (Wang *et al.*, 2015b). Emissions of P from fossil fuels and biofuel were estimated annually for 1960 to 2007 (Wang *et al.*, 2015a), which were extended to other years of simulations. Natural emissions of P from mineral dust, primary biogenic aerosol particles, sea salt and volcanoes were assumed to be constant (Wang *et al.*, 2015a). All N and P emissions from fossil fuels, biofuel and agricultural activities were assumed to be constant throughout each year without seasonal variation. Monthly 0.5°×0.5° gridded emissions by natural or anthropogenic (deforestation) burning of biomass were generated for 1997-2013 from the GFED4.1 inventory (Giglio *et al.*, 2013) and for other years from the ACCMIP inventory (Lamarque *et al.*, 2010). Emissions from biomass burning for 2030, 2050 and 2100 were assumed to be the same as the averages for 2010-2013. We only analyzed the changes of future N and P deposition from anthropogenic sources due to the lack of estimates of natural emissions, but both natural and anthropogenic sources were included for evaluating modeled N and P deposition

against measurements.

2.2. Observed N and P deposition rates and P concentrations

To evaluate the modeled N and P deposition rates, we used three observational data sets (**Figure S1**), including (i) a recent global data set of wet N deposition rates measured during 2002-2006 (Vet *et al.*, 2014), (ii) a recent global data set of total P deposition rates measured during 1960-2010 (Tippling *et al.*, 2014), and (iii) a recent global data set of surface P deposition concentrations measured during 1960-2008 (Mahowald *et al.*, 2008). Dry N deposition was not evaluated due to the lack of data, similar to previous studies (Larmarque *et al.*, 2005; Dentener *et al.*, 2006). Before using these observational data for model evaluation, we have further collected data to increase coverage of wet N deposition data in South America and Africa, removed some data of total P deposition with a high potential for contamination, and divided the measured surface P concentrations into short-term and long-term measurements. A full description is provided in the **Supporting Information**.

2.3. Additional C fixation attributable to N and P deposition

2.3.1. A stoichiometric method

A stoichiometric mass balance approach was used to estimate the change in C storage attributable to N and P deposition over global forests, based on the fraction of deposited nutrients retained in the ecosystems and incorporated into biomass and soil carbon pools (Nadelhoffer *et al.*, 1999; Cleveland *et al.*, 2013; de Vries *et al.*, 2014; Wieder *et al.*, 2015). We distinguished between four biomass C pools (leaves, stems, fine roots and coarse roots; each with different stoichiometry) and one soil C pool. Five types of forests are considered, namely deciduous broadleaf, deciduous needle-leaf, evergreen broadleaf, evergreen needle-leaf and mixed forests. The global land cover data set at a spatial resolution of 1 km (Hansen *et al.*, 2000) for the year 2010, as a product of Moderate Resolution Imaging Spectroradiometer (MODIS), was used to map these five types of forests. Forest areas have changed significantly since 1850 (Foley *et al.*, 2005; Houghton *et al.*, 2003). Here, we applied the fixed forest cover map by Hansen *et al.* (2000) in the calculation of $\Delta C_{v\ dep}$ throughout the period of 1850-2100. The uncertainty induced by assuming a fixed forest cover map on $\Delta C_{v\ dep}$ is quantified in **Section 3.7**. To do this, we re-calculated $\Delta C_{v\ dep}$ with the variable forest cover map for 1850-2010 according to the reconstruction of (Peng *et al.*, 2017) and the fraction of five types of forests within each 1°×1° grid from Hansen *et al.* (2000).

We assumed that in 1850 the forest C stocks were in equilibrium with the pre-industrial N and P deposition levels (i.e. $\Delta C_{v\ dep} = 0$), so that only the change in N and P deposition relative to the background levels can cause an extra forest C storage, allowing our estimates to cover the additional N and P emissions from fossil fuels and biofuel burning, atmospheric NH_3 and NO_x emissions from agriculture, and change in N and P emissions from biomass burning compared to 1850. Hence our analysis included the wind export of P from croplands and savanna to forests through fire emissions and atmospheric transport. It should be noted that direct anthropogenic effects on fires (*e.g.*, fire suppression and land use change) and indirect anthropogenic effects (*e.g.*, changes in climate affecting fire regimes) were not explicitly distinguished in the historical fire emission inventory we used (Giglio *et al.*, 2013). In addition, although our calculation of

193 $\Delta C_{v\ dep}$ covers C storage due to N and P from anthropogenic fires, we did not try to estimate the C
194 emissions from these anthropogenic fires which are always termed as part of C emissions from land-use
195 change in global C budget (Le Quere *et al.*, 2016). However, we did not account for the change of
196 atmospheric CO_2 concentrations, climate and forest cover change (Hansen *et al.*, 2013).
197 In each pixel at a spatial resolution of 1°×1°, additional forest C storages supported by anthropogenic N or
198 P deposition ($\Delta C_{v\ dep}$, where v stands for either N or P) were expressed as:

199 $$\Delta C_{N\ dep_i}(t) = f_{N_{veg}} a_{N_i} s_{N_i} [d_N(t) - d_N(1850)] \quad (1)$$

200 $$\Delta C_{P\ dep_i}(t) = f_{P_{veg}} a_{P_i} s_{P_i} [d_P(t) - d_P(1850)] \quad (2)$$

201 where i is biomass pool (i = 1 for leaves, 2 for stems, 3 for fine roots and 4 for coarse roots), f_{Nveg} and f_{Pveg}
202 are the retention fractions of deposited N and P in biomass pools, respectively, a_{Ni} and a_{Pi} are the allocation
203 fractions of N and P in each pool, respectively, s_{N_i} and s_{P_i} are the C:N and C:P stoichiometric ratios,
204 respectively, and $d_N(t)$ and $d_P(t)$ are the deposition rates of N and P for year t, respectively. All deposition
205 fields and land cover fractions were re-interpolated to the 1°×1° grid for the calculation of $\Delta C_{v\ dep}$.
206 Similarly, in each pixel, the $\Delta C_{v\ dep}$ realized in soil were expressed as:

207 $$\Delta C_{N\ dep_{soil}}(t) = f_{N_{soil}} s_{N_{soil}} [d_N(t) - d_N(1850)] \quad (3)$$

208 $$\Delta C_{P\ dep_{soil}}(t) = f_{P_{soil}} s_{P_{soil}} [d_P(t) - d_P(1850)] \quad (4)$$

209 where f_{Nsoil} and f_{Psoil} are the retention fractions of N and P in soil, respectively, and $s_{N_{soil}}$ and $s_{P_{soil}}$ are the C:N
210 and C:P stoichiometric ratios in soil biota, respectively.

211 There are two limitations in our approach. First, like de Vries *et al.* (2014), we approximate a time scale of
212 10-20 years for the $\Delta C_{v\ dep}$, because ecosystems take time to sequester C in forest biomass and soil after an
213 initial disturbance (Goulden *et al.*, 2011), such as the level of N and P deposition for most of the global
214 forests. It should be noted that our stoichiometric mass-balance model cannot resolve processes governing
215 the C storage changes attributed to deposition on shorter timescales. It is likely that the instantaneous effect
216 at the early stage of forest succession (e.g., less than 5 years) is lower, due to enhancement of soil C
217 decomposition by N deposition (Goulden *et al.*, 2011). Second, different turnover times of the plant and
218 soil pools should influence the C response to deposition, which is not included in our model. According to
219 de Vries *et al.* (2014), the C storage in the woody biomass (stem and coarse root) determines C
220 sequestration by forest trees, while the C storage in the non-woody biomass (leaves and fine root), which is
221 fast-turnover (Iversen *et al.*, 2017), determines C sequestration in soil. We estimated the sum of them based
222 on the allocation of the deposited nutrient in different pools measured at a time scale of around 2-9 years
223 (Schlesinger, 2009). At longer time periods, the C sequestration is determined by other disturbances, such
224 as forest fires and forest harvesting, which is not considered in our study. More knowledge gained in
225 database analyses for nutrient use in the tree growth (*e.g.*, Sardans and Peñuelas, 2013, 2015) would enable
226 us to better understand these processes in future process-based ecosystem models.

Although $\Delta C_{v\ dep}$ account for C storage supported by deposited nutrients on timescales of 10-20 years (de Vries *et al.*, 2014), it should be noted that a fraction of deposited N and P may still contribute to $\Delta C_{v\ dep}$ beyond the 10-20 year timeframe. This impact is small for $\Delta C_{N\ dep}$, because a large fraction of N is lost by denitrification or leaching. The impact for $\Delta C_{P\ dep}$, however, is not negligible, because P is mostly fixed by the soil and is less prone to loss. We estimated $\Delta C_{P\ dep}$ by fixing an "effective fraction" of the deposited P ($f_{P_{fix}}$) to account for this impact (see **Section 2.3.2**).

All parameters were determined with central values and uncertainty ranges (see **Section 2.3.2**, **2.3.3**, and **2.3.4**). In brief, the parameters f_{Nveg}, f_{Pveg}, a_i, s_{Ni}, s_{Pi}, f_{Nsoil} and f_{Psoil} were derived for deciduous broadleaf, deciduous needle-leaf, evergreen broadleaf, evergreen needle-leaf and mixed forests; parameters values and their uncertainty ranges are summarized in **Table 1**. Uncertainties in the modeled deposition rates (d_N and d_P) were derived from a comparison with the available observation data sets (see **Section 3.2**).

Table 1. Parameters used to estimate carbon fixation due to anthropogenic N and P deposition in forests. The 95% confidential intervals adopted as the lower and upper estimates for each parameter applied in our Monte Carlo simulations are in parentheses.

Forest type	Evergreen needleleaf forest	Evergreen broadleaf forest	Deciduous needleleaf forest	Deciduous broadleaf forest	Mixed forest
C:N (g C: g N)					
Leaves	42 (34-50)	21 (17-25)	50 (40-60)	21 (17-25)	28 (22-34)
Stems	250 (200-300)	150 (120-180)	250 (200-300)	175 (140-210)	175 (140-210)
Fine roots	78 (62-94)	78 (62-94)	41 (33-49)	41 (33-49)	41 (33-49)
Coarse roots	250 (200-300)	150 (120-180)	250 (200-300)	175 (140-210)	175 (140-210)
Soil	31 (28-35)	16 (14-18)	20 (18-21)	19 (18-20)	19 (18-20)
C:P (g C: g P)					
Leaves	408 (326-490)	400 (320-480)	405 (324-486)	333 (266-400)	278 (222-334)
Stems	3750 (3000-4500)	2250 (1800-2700)	3750 (3000-4500)	2625 (2100-3150)	2625 (-)
Fine roots	1170 (936-1404)	1020 (816-1224)	615 (492-738)	615 (492-738)	615 (492-738)
Coarse roots	3750 (3000-4500)	2250 (1800-2700)	3750 (3000-4500)	2625 (2100-3150)	2625 (2100-3150)
Soil	1030 (459-2312)	169 (134-214)	318 (214-472)	391 (306-500)	254 (214-300)
Retention fractions of N and P in plants					
f_{Nveg}	0.23 (0.14-0.30)	0.15 (0.10-0.20)	0.23 (0.14-0.30)	0.23 (0.14-0.30)	0.23 (0.14-0.30)
f_{Pveg}	0.05 (0.016-0.22)	0.09 (0.027-0.36)	0.05 (0.016-0.22)	0.05 (0.016-0.22)	0.05 (0.016-0.22)
Retention fractions of N and P in soil					
f_{Nsoil}	0.52 (0.26-0.78)	0.15 (0.10-0.20)	0.52 (0.26-0.78)	0.52 (0.26-0.78)	0.52 (0.26-0.78)
f_{Psoil}	0.13 (0.038-0.50)	0.09 (0.03-0.36)	0.13 (0.038-0.50)	0.13 (0.038-0.50)	0.13 (0.038-0.50)
Allocation fraction of N (a_{Ni})					
Leaves	0.42	0.56	0.42	0.49	0.46
Stems	0.34	0.22	0.34	0.33	0.34
Fine roots	0.16	0.17	0.16	0.11	0.13

Coarse roots	0.08	0.05	0.08	0.07	0.07
Allocation fraction of P (a_{Pi})					
Leaves	0.32	0.63	0.28	0.50	0.35
Stems	0.40	0.19	0.42	0.32	0.40
Fine roots	0.19	0.13	0.20	0.11	0.16
Coarse roots	0.09	0.04	0.10	0.07	0.09

Sensitivity tests were performed to quantify the influence of the major parameters on the $\Delta C_{v\,dep}$ by N and P (see **Section 3.4**). Finally, Monte Carlo simulations were applied to estimate the central values of $\Delta C_{v\,dep}$ in global forests and to estimate their uncertainties in each pixel at a spatial resolution of 1°×1°. In brief, the model was run 10000 times by drawing input parameters from uniform or normal uncertainty distributions of model parameter and N- and P-deposition rates. The medians and 95% confidence intervals (CI) were used to represent the central estimate and the associated uncertainty, respectively, based on the Monte Carlo simulations.

2.3.2. Retention of N and P in the ecosystems

Schlesinger (2009) reported a median N retention fraction of 23% (with an interquartile range of 14-30%) for biomass pools (f_{Nveg}) and 52% (with an interquartile range of 26-78%) for soils (f_{Nsoil}) in boreal and temperate forests. De Vries *et al.* (2007) suggested a lower N-retention fraction of 15% (with a 90% uncertainty range of 10-20%) for both f_{Nveg} and f_{Nsoil} in tropical forests. We adopted these median estimates and their uncertainty ranges. The non-retained fraction of deposited N lost by leaching, volatilization and denitrification is not explicitly modeled.

Evidence suggests that N inputs from atmospheric deposition can be taken up by forest canopies (Sievering *et al.*, 2007; Gaige *et al.*, 2007; Sparks, 2009). De Vries *et al.* (2014), however, suggested that the effect of uptake of N by canopies on C fixation is likely to be small, because a small fraction of canopy-retained N is absorbed and used in leaves. Gaige *et al.* (2007) suggested that denitrification and nitrification do not occur in the canopy, despite a high retention fraction of N deposition in the canopy. Sparks (2009) suggested that foliar uptake of reactive N should be considered separately from soil-deposited N, but pointed out that it is difficult to link canopy uptake of N directly to assimilation. Dail *et al.* (2009) found that only 3-6% of the labeled ^{15}N recoverable in plant biomass was recovered in live foliage and bole wood and that tree twigs, branches and bark were the major sinks (50%) after 2 years of NH_4NO_3 addition. We therefore did not account for this process in our central case, following the suggestion by de Vries *et al.* (2014), but discuss the potential impact in a sensitivity test in **Section 4.2**.

The fate of deposited P in ecosystems differs from that of N. First, P is less mobile than N in soils (Aerts and Chapin, 2000), so the fractional P loss by leaching is smaller than for N. Second, denitrification has no counterpart for gaseous P loss to the atmosphere. Third, the physical fixation of P and its eventual occlusion in soil reduces the availability of deposited P to leaching and uptake by plants and microbes. The fate of deposited P in forests has unfortunately not yet been measured, to the best of our knowledge, and

was estimated in our study based on two assumptions. First, we assumed that 10% of the deposited P was directly lost by runoff as Sattari *et al.* (2012) assumed for fertilizer P. Second, by assuming that P deposition input to soil is much smaller than the actual stocks of labile and stable P in soil and thus does not affect the stock size, we approximated the fixation of an "effective fraction" of deposited P ($f_{P_{fix}}$), corresponding to the net transfer of P between 'labile' and 'stable' forms, based on transfer coefficients (μ_{SL} and μ_{LS}) between stable and labile P:

$$f_{P_{fix}} = 1 - \mu_{SL}/\mu_{LS} \quad (5)$$

We used μ_{SL} and μ_{LS} to derive a central estimate of $f_{P_{fix}}$ (80%) but a wide range of uncertainty (20% to 94%) as recommended by Sattari *et al.* (2012). We also assumed that the fraction of ecosystem-retained P taken up by plants ($f_{P_{uptake}}$) was the same as that of N, at 30% for boreal and temperate forests and 50% for tropical forests (Schlesinger, 2009; de Vries *et al.*, 2007), due to lack of direct measurements of the fraction of ecosystem-retained P taken up by plants. We then derived the retention of P in vegetation ($f_{P_{veg}}$) and soil ($f_{P_{soil}}$) using $f_{P_{fix}}$, $f_{P_{loss}}$ and $f_{P_{uptake}}$:

$$f_{P_{veg}} = (1 - f_{P_{loss}})(1 - f_{P_{fix}})f_{P_{uptake}} \quad (6)$$

$$f_{P_{soil}} = (1 - f_{P_{loss}})(1 - f_{P_{fix}})(1 - f_{P_{uptake}}) \quad (7)$$

Código de campo cambiado

Código de campo cambiado

We estimated that $f_{P_{veg}}$ was 5.4% (1.6-22% as the uncertainty range) and $f_{P_{soil}}$ was 13% (3.8-50% as the uncertainty range) in boreal and temperate forests and that $f_{P_{veg}}$ was 9.0% (2.7-36% as the uncertainty range) and $f_{P_{soil}}$ was 9.0% (2.7-36% as the uncertainty range) in tropical forests (**Table 1**).

2.3.3. Allocation of N and P in plants

We used the values of a_{Ni} diagnosed by de Vries *et al.* (2014) for deciduous broadleaf, evergreen broadleaf and needleleaf forests. The a_{Ni} averaged over deciduous broadleaf and needleleaf forests was applied for mixed forests (**Table 1**). The uncertainty associated with a_{Ni}, however, was not provided and was estimated below. The C:N ratio differs for woody (stem and coarse root) and non-woody (leaf and fine root) pools, so the assumption that uncertainties in a_{Ni} are the same as the uncertainties associated with the fraction of N allocated to the woody component is reasonable. A meta-analysis of ^{15}N addition experiments suggested that 53% of total N uptake is allocated to woody biomass (Templer *et al.*, 2012), compared to 25% reported by Nadelhoffer *et al.* (1999). This latter low value is 7-40% lower than that used in our study, and the high value is 26-96% higher than the central value used in our study (**Table 1**). We accordingly applied two half normal distributions to cover the uncertainty of a_{Ni}.

We are not aware of any experiment measuring the allocation of deposited P to different biomass pools, so we derived the allocation fractions of P and their uncertainties from the allocation of N and the stoichiometric ratios of these two elements as:

$$a_{P_i} = \frac{a_{N_i} \cdot s_{N_i}/s_{P_i}}{\sum_{i=1}^{4}\left(a_{N_i} \cdot s_{N_i}/s_{P_i}\right)} \quad (8)$$

where s_{Ni} and s_{Pi} are the C:N and C:P stoichiometric ratios, respectively, in each pool of the plant.

2.3.4. C:N and C:P stoichiometric ratios in different pools

C:N and C:P stoichiometric ratios in soil and their 95% CI were derived from a global data set of the nutrient composition of soil (Xu *et al*., 2013). The median C:N and C:P stoichiometric ratios of leaves, stems, fine roots and coarse roots were obtained from Cleveland *et al.* (2013). Wang *et al*. (2010) suggested that the minimum and maximum of C:N and C:P stoichiometric ratios were ±20% relative to the means, which we applied as uncertainties for s_{N_i} and s_{P_i}.

2.4. Maximum and minimum effects of N and P deposition

The change in C fixation due to nutrients addition in an ecosystem can be approximated based on the most limiting element (Vitousek *et al*, 1984, 2010), but the stoichiometric mass balance approach we used could not identify the most limiting element. Therefore, we estimated the maximum and minimum effects of $\Delta C_{v\,dep}$ due to anthropogenic N and P deposition to characterize the degree of limitation by one of the two elements. Accordingly, the minimum effects of anthropogenic N and P deposition yields a lower estimate as:

$$\Delta C_{v\,dep}^{min} = \min[\Delta C_{N\ dep}, \Delta C_{P\ dep}] \quad (9)$$

and the maximum effects of N and P deposition yields an upper estimate as:

$$\Delta C_{v\,dep}^{add} = \max[\Delta C_{N\ dep}, \Delta C_{P\ dep}] \quad (10)$$

The minimum and maximum effects calculated here should be interpreted with caution. First, the minimum effect is based on a hypothesis that the element with a lower capacity to fix C by deposition is more limiting and that there is no additional source of this element than atmospheric deposition to support a larger C storage. The difference between the effect by an element alone and the minimum effect denotes the limitation by the other element that is enhanced by the deposition. Second, the maximum effect is based on a hypothesis that the element with a higher capacity to fix C by deposition is more limiting and there is enough of the other element to allow for the largest C storage. The difference relative to the effect by an element alone denotes the limitation by the other one that is alleviated by the deposition. Regarding uncertainties in the limitations by N and P, the combined effect of N and P deposition should fall between the minimum and maximum effects. Although we cannot rule out that there are synergistic "*additive*" effects (Elser *et al.*, 2007) as well as strictly negative effects (Penuelas *et al.*, 2013), such effects are rather unlikely to occur in wide ranges of ecosystems and deposition loads. In addition, difference between the maximum and minimum effect quantifies an imbalance between N and P induced by the deposition providing that other sources of N and P were held constant. However, it should be noted that our calculation does not account for the interaction between N and P cycles implied by recent studies. For example, increasing N deposition can affect availability, uptake and using efficiency of P by altering mycorrhizal activity, phosphatase enzymes and soil properties (Compton and Cole, 1998; Rowe *et al.*, 2008; Marklein and Houlton, 2012; Lü *et al.*, 2013).

3. Results

3.1. N and P emissions

Natural and anthropogenic global emissions of N and P were estimated or derived for the past time slices in

1850-1990, for each year in 1997-2013 and for the future time slices in 2030-2100 (Figure 1). Total reactive-N emissions increased from 35 Tg N yr^{-1} in 1850 to an average of 104 Tg N yr^{-1} for 1997-2013, and were predicted to reach 83 and 114 Tg N yr^{-1} by 2100 under the RCP4.5 and RCP8.5 scenarios, respectively. N emissions as the oxidized (NO_x) and reduced (NH_3) forms are listed in **Table S3**, which are close to previous estimates (Holand *et al.*, 1997; Galloway *et al.*, 2004; Lamarque *et al.*, 2005; Dentener *et al.*, 2006; Paulot *et al.*, 2013). The main drivers of the increase in historical N emissions were a rapid rise in the use of fossil fuels, both the expansion and intensification of agricultural fertilization and an increase in the number of livestock (Schlesinger, 2009). N emissions from fossil fuel, biofuel and agricultural activities increased from 5.6 Tg N yr^{-1} in 1850 (Lamarque *et al.*, 2010) to 60 Tg N yr^{-1} in 2005 (Klimont *et al.*, 2013). The increase in reactive-N emissions was equivalent to twice the background N emissions in 1850. The emissions of P increased from 2.6 to 4.0 Tg P yr^{-1} from 1850 to 2013, equivalent to a 57% increase relative to the background 1850 emissions. 47%, 25% and 28% of the increase in P emissions were from increases in emissions from fossil fuels, biofuel and deforestation fires, respectively. The N:P ratio in the emissions nearly doubled from 25 (on a molar basis) in 1850 to 48 in 2013 due to a faster growth of N than P emissions as outlined in a previous study (Peñuelas *et al.*, 2013).

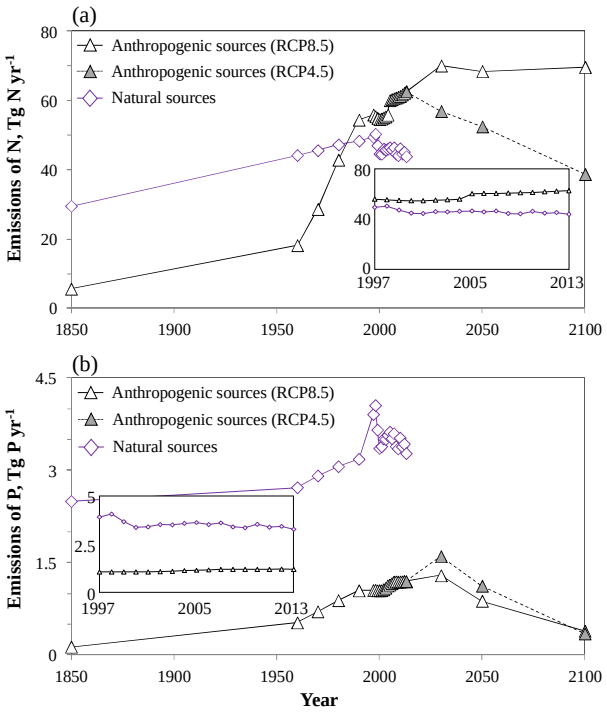

Figure 1. (a) Global atmospheric N emissions. Anthropogenic sources include fossil fuels, biofuel and agricultural activities. Natural sources include NO_x and NH_3 emissions from biomass burning, NO_x and NH_3 emissions from soil, and NH_3 emissions from oceans. (b) Global atmospheric P emissions. Anthropogenic sources include fossil fuels and biofuel. Natural P sources include biomass burning, dust, sea salt, volcano particles and primary biogenic aerosol particles. The inset demonstrates the inter-annual recent variation over the period 1997-2013.

The future emissions of N differed considerably between the RCP4.5 and RCP8.5 scenarios, but the emissions of P were similar. NH_3 emissions in 2100 will be 54% under the RCP8.5 than the RCP4.5 scenario, due to increased agricultural activities needed to meet the food demand of a larger global population (Lamarque *et al.*, 2011; Riahi *et al.*, 2011). In contrast, 70% of P emissions from fossil fuels and biofuel were expected to be removed, due to a high penetration rate of clean technology in the industrial and residential sectors under both the RCP4.5 and RCP8.5 scenarios, leading to a slight difference between the two scenarios.

3.2. Spatial distributions of N and P deposition

The pre-industrial (1850) and present (1997-2013) spatial distributions of N and P deposition are shown in Figure 2. Dentener *et al*. (2006) recommended 1000 mg N m^{-2} yr^{-1} as a "critical load" threshold for plant sustainability, and rates above this threshold may lead to changes in ecosystemic functioning. The deposition rate of N for 1997-2013 also exceeded 1000 mg N m^{-2} yr^{-1} in large areas of India (72%), China (45%) and Europe (26%). The deposition rate of P for 1997-2013 exceeded 100 mg P m^{-2} yr^{-1} in the Indo-Gangetic region of India due to a high use of biofuels (*e.g.*, dung cake is widely used for cooking) and in the Congo Basin in Central Africa due to deforestation (Chen *et al.*, 2010).

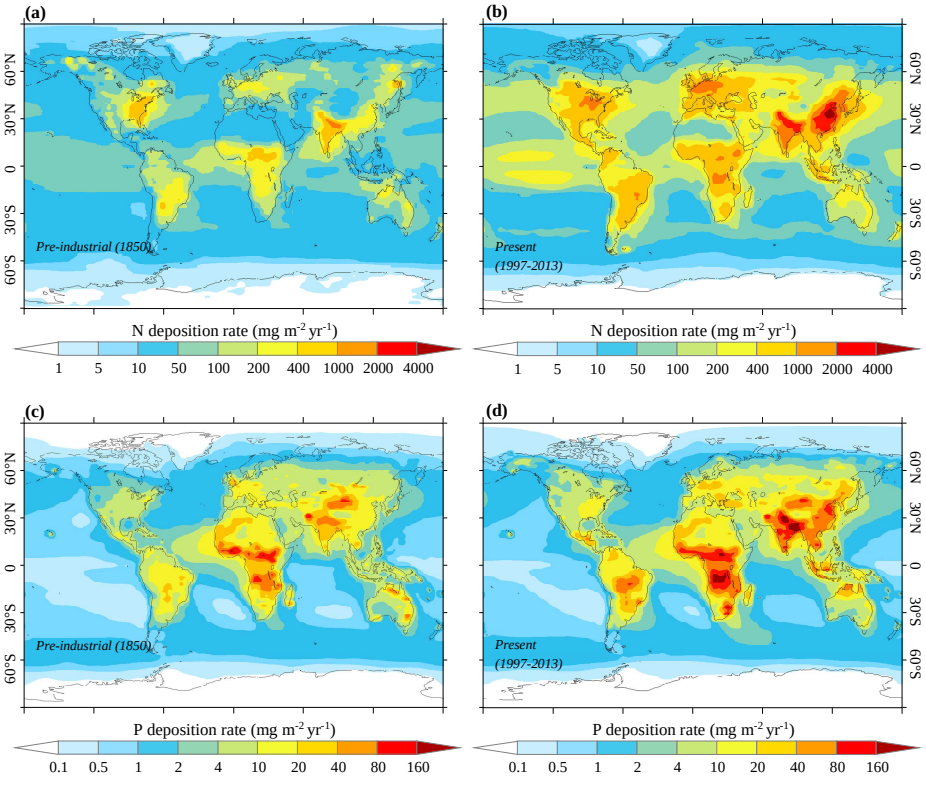

Figure 2. (a,b) Spatial distribution of N deposition in 1850 (a) and 1997-2013 (b). (c,d) Spatial distribution of P deposition in 1850 (c) and 1997-2013 (d).

The modeled spatial distributions of N wet and P total deposition rates were evaluated by measurements at the forest sites and at all sites (Figure 3). The comparison indicated that our model broadly captured the spatial patterns in the observed deposition rates of N and P. A normalized mean bias (difference between the geometric mean of the model minus the geometric mean of the measurements relative to the latter) was used to quantify the bias. A statistical analysis show that 50% of the data were subject to a bias of -25% to 50% in the modeled wet N deposition and -4% to 164% in the modeled total P deposition relative to observations (**Figure S2**). We addressed the potential uncertainty by scaling the modeled N deposition rate by a fixed factor that followed a normal distribution, with a mean of 1.2 and a standard deviation of 0.6, and the modeled P deposition by a fixed factor that followed a normal distribution, with a mean of 1.6 and a standard deviation of 1.0, which were derived from the frequency distribution of the model bias (**Figure S2**). The scaled deposition rates of N and P were used in the calculation of $\Delta C_{v\,dep}$. The data for observed N wet deposition enabled us to further evaluate the modeled wet deposition of N in the oxidized (NO_3) and reduced (NH_4) forms by region (**Figure S3**).

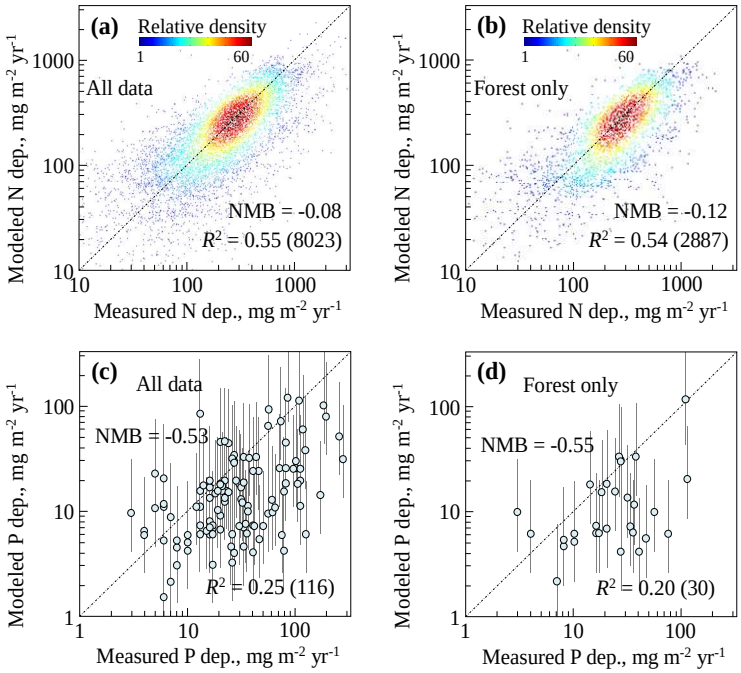

Figure 3. Comparison of modelled and observed deposition of wet N (a,b) and total P (c,d). (a,c) show all data and (b,d) show measurements over forests only. In (a,b), colours show the relative density of data. In (c,d), the error bars show the uncertainty associated with emissions of P from different sources as estimated by Wang *et al.* (2015a). Coefficient of correlation (R^2) and normalized mean bias (NMB) of log-transferred deposition rates are given in each panel with the number of data in bracket.

Figure S4 shows a comparison of our modeled surface concentrations of P for particles of the same size

with the observational data used by Mahowald *et al.* (2008). These discrete sampling measurements were temporally variable, so we focused on comparing the modeled P concentrations with long-term measurements. It shows that including a large contribution of P from combustion sources can reduce the normalized mean bias from -31% to -11%, while our estimates were subject to uncertainty errors between -73% to 105% as 95% CIs in the estimation of P emissions from different sources (Wang *et al*., 2015a).

3.3. Temporal trends of N and P deposition in forests

Figure 4 shows the temporal trends of N and P deposition in forests in various regions from 1850 to the present. The increase in the rate of N deposition in forests from 1850 to the present ranged from 1.5- to 7-fold by region. The rate of P deposition in forests increased by 1- to 3.5-fold from 1850 to the present, due to a smaller contribution of anthropogenic source than for N. The deposition of N and P in North American and European forests both peaked in the 1980s or 1990s. Specifically, the deposition rates of N and P in European forests peaked in the 1980s and 1990s, respectively. The rate of N deposition in North American forests peaked in 1990, but the rate of P deposition continued to increase. The increase in the deposition of P in North American forests was mainly due to an increase in emissions from biomass burning during the last two decades (Westerling, *et al*. 2006). This increase was captured by the GFED4.1 and ACCMIP inventories (Lamarque *et al*., 2010; Giglio *et al*., 2013) used in our study. **Figure S5** shows that this increasing trend was also confirmed by three other inventories for biomass burning. The rate of N deposition in Siberian forests had a trend similar to that of European forests due to the atmospheric transport of N from Europe, but the rate of P deposition was mainly governed by the variability of wildfires. The rate of N deposition in the forests in Australia and New Zealand increased continuously, but the rate of P deposition began to decline in Australia after 1980 due to the replacement of P-rich fuels (coal) with P-poor fuels (petroleum or natural gas) (IEA, 2013).

The rate of N deposition in East Asian forests was 7-fold higher in 2010 than 1850 and more than 4-fold in Southern/Southeastern forests. Total N emissions were highest in China and India, but NO_x emissions had increased more in China from 1990 to 2010 by 150%, compared to 80% in India, due to a faster growth in fleet vehicle in China (Granier *et al*., 2011).

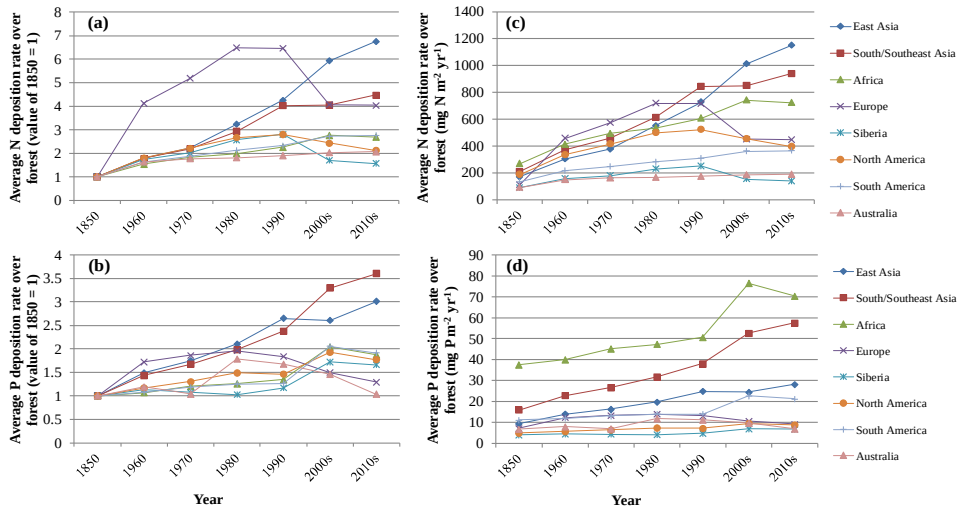

Figure 4. Temporal trends of N (a,c) and P (b,d) deposition rate over forests by region. (a,b) show the values relative to 1850, while (c,d) show absolute values. The data for 2000s represent an average over 1997-2004 and the data for 2010s represent an average over 2005-2013.

The rate of P deposition in East Asian forests increased 2.5-fold from 1850 to 1990 and stabilized after 1990. **Figure S6** shows the inter-annual variability of N- and P-deposition rates in the forests in East Asia and South/Southeast Asia from 1997 to 2013. The rate of N deposition increased continuously, but the rate of P deposition remained more stable in these two regions. The increase in the rate of N deposition was driven by the increase of in the use of fossil fuels and in agricultural activities. The rate of P deposition, however, was driven by emissions from fossil fuels, biofuel and biomass burning. The increase in fires and biomass burnt during the 1997-1998 El Niño led to a peak in the P-deposition rate in the forests in East Asia and South/Southeast Asia (van der Werf *et al.*, 2004).

Figure 5 shows the temporal trends of the N:P deposition ratio (on a molar basis) in forests by region. The ratio peaked in around 1990 in the forests in Europe, Siberia and North America and then decreased due to a decline in the deposition of N and an increase in the deposition of P due to increasing wildfires. The N:P deposition ratio in the forests did not vary greatly in the forests in South/Southeast Asia, Africa and South America, because the rates of N and P deposition increased at similar rate. In contrast, the N:P deposition ratio increased continuously in the forests in East Asia due to rapid increases in the emission and deposition of N in this region. The N:P deposition ratio in the 2010s was significantly larger in the forests in Europe, North America and East Asia than in the other regions.

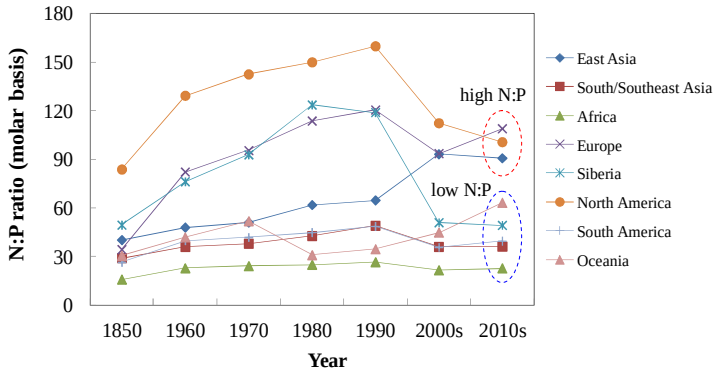

Figure 5. Temporal evolution of N:P ratio in the deposition over forests by region. The data for 2000s represent an average over 1997-2004 and the data for 2010s represent an average over 2005-2013.

3.4. Forest C fixation due to anthropogenic N and P deposition

Based on the maps of N and P deposition, we calculated the global forest $\Delta C_{v\,dep}$ using the stoichiometric mass balance approach. Figure 6 shows that, for control values of the parameters, anthropogenic deposition of N and P for 1997-2013 led to global $\Delta C_{v\,dep}$ (median ± 90% CI from Monte Carlo simulations) of 0.27 ± 0.13 and 0.054 ± 0.10 Pg C yr^{-1}, respectively. A total of 10 000 Monte Carlo simulations were run by randomly entering parameters from a prior uniform or normal distribution of parameters. The frequency distributions of global $\Delta C_{v\,dep}$ by anthropogenic N and P deposition averaged for 1997-2013 are shown in **Figure S7**. Some parameters were uniformly or normally distributed, but the output was nearly normally distributed for $\Delta C_{N\,dep}$ ($P > 0.1$) and log-normally distributed for $\Delta C_{P\,dep}$ ($P > 0.2$). For a global terrestrial C sink of 3.1 ± 0.9 Pg C yr^{-1} averaged for 2006-2015 (Le Quere *et al.*, 2016), $\Delta C_{v\,dep}$ by anthropogenic N and P deposition contributed 8.7% and 1.7% to the terrestrial C sink, respectively.

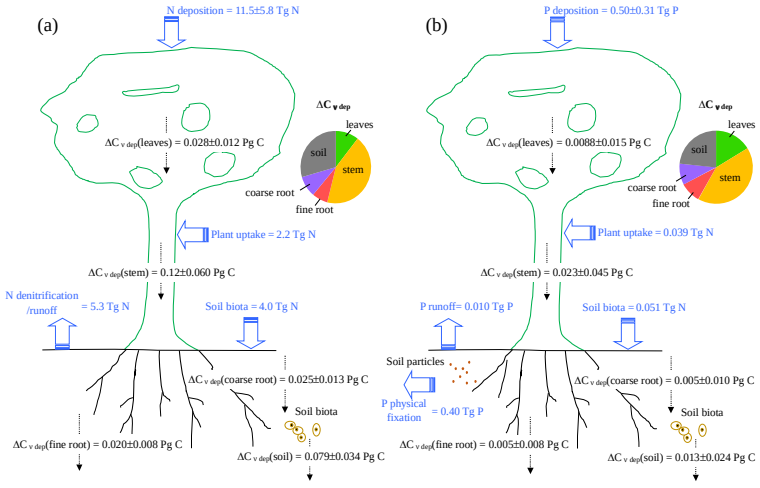

Figure 6. Anthropogenic N and P deposition over forest and $\Delta C_{v\,dep}$ due to anthropogenic N and P deposition per year as an average over 1997-2013. (a) for N and (b) for P. Uncertainty of the modeled N

and P deposition as standard deviations is derived from a comparison with observations. Uncertainty of the $\Delta C_{v\ dep}$ as 90% CI is derived from Monte Carlo simulations. The pie charts show the distribution of $\Delta C_{v\ dep}$ among five pools.

Figure 6 also shows that 43% of $\Delta C_{N\ dep}$ was stored in stems, followed by soil (29%), leaves (11%), coarse roots (9%) and fine roots (7%). Similarly, stems (42%) were the most important storage pool for $\Delta C_{P\ dep}$. In addition, we performed sensitivity tests using the lower or upper bounds of the parameters to investigate the influences on our estimated $\Delta C_{N\ dep}$ (**Table 2**). It shows that the major parameters influencing $\Delta C_{v\ dep}$ by N or P include the retention ratios of N in vegetation and soils, the physical fixation of P by soil, the fraction of N and P allocated to woody biomass, and the C:N and C:P stoichiometric ratios in each pool. $\Delta C_{P\ dep}$ was generally associated with a far higher uncertainty than $\Delta C_{N\ dep}$. Most importantly, we assumed that a large fraction of P (80%) was fixed by the soil as inorganic P, which is unavailable for C storage (Walker and Syres, 1976). Assuming a weaker or stronger fixation of P by soils, which influences estimates of $\Delta C_{v\ dep}$ by P the most, however, led to a difference in $\Delta C_{P\ dep}$ from -70% to +300%.

Table 2. Global forest $\Delta C_{v\ dep}$ due to anthropogenic N and P deposition over 1997-2013. Sensitivity tests were run to compare with a standard run with central values of parameter. The sensitivity tests include high or low retention fraction of N in vegetation and soil; weak or strong fixation of P by soil particles; high or low fraction of N and P allocated to the woody part; high or low C:N and C:P stoichiometric ratios. Values in brackets show the percentage changes relative to the standard run.

	Leaf	Stem	Fine root	Coarse root	Soil	Woody	Total
Forest $\Delta C_{v\ dep}$ by N deposition over 1997-2013 (Pg C yr^{-1})							
Standard run	0.028	0.117	0.020	0.025	0.079	0.142	0.269
High retention fraction	0.037	0.153	0.026	0.033	0.107	0.186 (+31%)	0.356 (+32%)
Low retention fraction	0.018	0.073	0.013	0.016	0.042	0.088 (-38%)	0.160 (-40%)
High woody fraction	0.021	0.168	0.014	0.037	0.079	0.205 (+45%)	0.320 (+19%)
Low woody fraction	0.034	0.079	0.022	0.017	0.079	0.097 (-32%)	0.232 (-14%)
High C:N ratio	0.034	0.140	0.024	0.030	0.079	0.170 (+20%)	0.307 (+15%)
Low C:N ratio	0.023	0.093	0.016	0.020	0.079	0.113 (-20%)	0.231 (-15%)
Forest $\Delta C_{v\ dep}$ by P deposition over 1997-2013 (Pg C yr^{-1})							
Standard run	0.009	0.023	0.005	0.005	0.013	0.028	0.054
Weak fixation by soil	0.035	0.091	0.020	0.020	0.051	0.111 (+300%)	0.218 (+300%)
Strong fixation by soil	0.003	0.007	0.002	0.002	0.004	0.008 (-70%)	0.016 (-70%)
High woody fraction	0.006	0.039	0.003	0.009	0.013	0.048 (+73%)	0.070 (+29%)
Low woody fraction	0.009	0.018	0.005	0.004	0.013	0.022 (-19%)	0.050 (-8%)
High C:P ratio	0.011	0.027	0.006	0.006	0.013	0.033 (+20%)	0.063 (+15%)
Low C:P ratio	0.007	0.018	0.004	0.004	0.013	0.022 (-20%)	0.046 (-15%)

3.5. Spatial patterns of N and P limitation

Increasing N from atmospheric deposition has been postulated to lead to a progressive emerging limitation of P (Vitousek *et al.*, 1984, 2010; Penuelas *et al.*, 2013). Figure 7 compares the forest area where $\Delta C_{N\ dep}$ is larger than $\Delta C_{P\ dep}$ between 1960 and the present (1997-2013) under different assumptions of the physical fixation of P by the soil. A faster increase in the deposition of N than P in forests close to industrialized regions had led to a growth in $\Delta C_{v\ dep}$ that is higher for N than for P. It should be noted that, as we did not account for other sources of N and P (*e.g.* weathering for P and nitrification for N), lower $\Delta C_{v\ dep}$ from N than P deposition is only one factor contributing to a limitation by P (Vitousek *et al.*, 1984, 2010; Penuelas *et al.*, 2012, 2013). Globally, the forests where $\Delta C_{N\ dep}$ is larger than $\Delta C_{P\ dep}$ in 1960 covered an area between 2.79 and 4.90 × 10^7 km^2, depending on the strength of soil P fixation. In these forests, additional supply of P from other sources (e.g., by mineralization) is needed to support $\Delta C_{v\ dep}$ by N. The forest area where $\Delta C_{N\ dep}$ is larger than $\Delta C_{P\ dep}$ had extended by 4% or 18% from 1960 to the present, which also depends on the strength of soil P fixation, mainly located in forests in South/Southeast Asia, East Asia, Europe and North America.

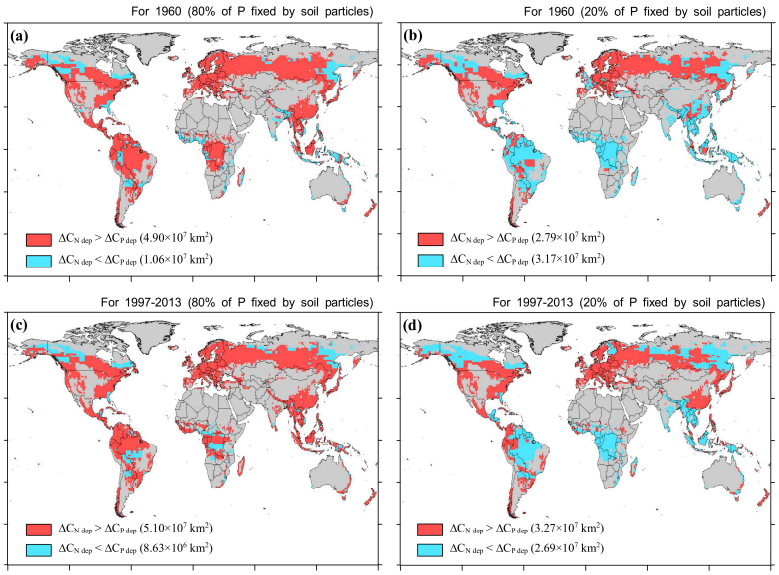

Figure 7. Spatial distribution of forest area where $\Delta C_{v\ dep}$ by anthropogenic N deposition is larger or smaller than $\Delta C_{v\ dep}$ by anthropogenic P deposition in 1960 (**a,b**) and as an average over 1997-2013 (**c,d**). In (**a,c**), the model assumes that 80% of the deposited P is fixed by soil particles, while (**b,d**) shows results in a sensitivity case where 20% of P is fixed by soil particles. The total areas where $\Delta C_{v\ dep}$ by anthropogenic N deposition is larger or smaller than $\Delta C_{v\ dep}$ by anthropogenic P deposition are in parentheses. Non-forest land areas are shown as grey.

3.6. Temporal trends of $\Delta C_{v\ dep}$ by N and P

Figure 8a shows the temporal trends of $\Delta C_{v\ dep}$ by N and P deposition alone for 1960-2100 under different physical fraction of P fixed in soil. $\Delta C_{v\ dep}$ by N peaked in 1990 and then declined due to reductions of N emissions and deposition in the forests in Europe and North America, but $\Delta C_{v\ dep}$ by P was projected to

increase by 2030 due to continuous increases in P emissions and deposition in South and Southeast Asia, Africa and South America under the RCP4.5 scenario. We also found that $\Delta C_{v\ dep}$ by N was much higher than $\Delta C_{v\ dep}$ by P in our central case where 80% of the P was fixed by soil, but they were very similar in a sensitivity test where only 20% of P was fixed by soil. $\Delta C_{v\ dep}$ by N for 2030, 2050 and 2100 was expected to be 28-60% higher under the RCP8.5 than the RCP4.5 scenario due to higher NH_3 emissions from agriculture. Difference in $\Delta C_{v\ dep}$ by P would be less than 15% due to a high control rate of industrial particulate emissions under both scenarios (Lamarque *et al.*, 2011) (**Figure S8**).

Based on $\Delta C_{v\ dep}$ by N and P in each 1°×1° grid, we calculated $\Delta C_{v\ dep}$ by N and P deposition together in the case of maximum or minimum effects from 1960 to 2100 (Figure 8b). $\Delta C_{v\ dep}$ was about 6-fold higher for maximum (0.28 Pg C yr^{-1} averaged for 1997-2013) than minimum (0.044 Pg C yr^{-1}) effects, highlighting the imbalance between N and P in the deposition. $\Delta C_{v\ dep}$ for maximum effects peaked at 0.29 Pg C yr^{-1} in 1990 and then decreased due to reductions of N emissions and deposition rates in the forests in Europe and North America. In a sensitivity test where 20% of P was fixed by soil, however, $\Delta C_{v\ dep}$ for maximum effect was predicted to increase continuously from 0.14 Pg C yr^{-1} in 1960 to 0.42 Pg C yr^{-1} in 2030 due to increases in both N and P deposition rates before 1990 and an increase in P deposition rate alone after 1990. **Figure S8** shows $\Delta C_{v\ dep}$ due to N and P together under the RCP8.5 scenario, where $\Delta C_{v\ dep}$ for maximum effect was expected to be 23-54% higher than under the RCP4.5 scenario.

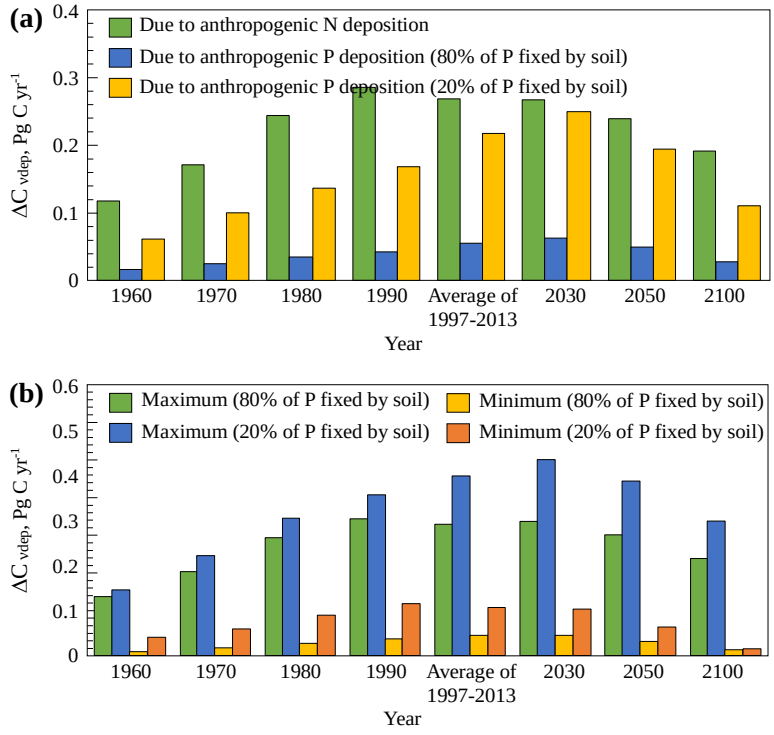

Figure 8. Temporal trends of global $\Delta C_{v\ dep}$ due to anthropogenic N and P deposition alone (**a**) and together as maximum or minimum effects (**b**) from 1960 to 2100. $\Delta C_{v\ dep}$ in a case where 80% of P is fixed by soil

is compared to a sensitivity case where 20% of P is fixed by soil. The $\Delta C_{v\ dep}$ for 2030, 2050 and 2100 are estimated based on the anthropogenic N and P deposition under the RCP 4.5 storyline.

3.7. **Impact of forest cover change on $\Delta C_{v\ dep}$**

In addition to the change of N and P deposition rates, the change of forest areas due to deforestation and afforestation influences $\Delta C_{v\ dep}$. **Table S4** shows the change of total forest areas, average N and P deposition fluxes over forests and $\Delta C_{v\ dep}$ estimated for the five types of forests using a reconstructed global data set of forest cover change from 1850 to 2010 (Peng *et al.*, 2017). Figure 9 compares the deposition fluxes and the $\Delta C_{v\ dep}$ for 1850 and 2010 with or without forest cover change by taking 1850 as a reference, whereas the results for 2010 are calculated using the forest cover map in 1850 or 2010. It shows that, if accounting for forest cover change, $\Delta C_{v\ dep}$ due to change in N and P deposition from 1850 to 2010 would decrease by 10% and 30%, respectively. Likewise, the deposition fluxes and $\Delta C_{v\ dep}$ for 1850 and 2010 are compared with or without the forest cover change by taking 2010 as a reference, whereas the results for 1850 are calculated using the forest cover map in 1850 or 2010 (**Figure S9**). Similarly, it shows that the forest cover change leads to a difference in $\Delta C_{v\ dep}$ by -6% and -19% for N and P, respectively.

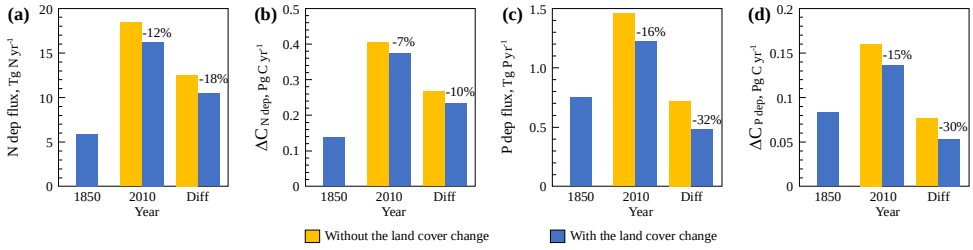

Figure 9. Comparison of global N deposition fluxes over forests (a), $\Delta C_{v\ dep}$ due to N deposition (b), P deposition fluxes over forests (c) and $\Delta C_{v\ dep}$ due to P deposition (d) in 1850 and 2010 and the difference between 1850 and 2010 (Diff) without or with the forest cover change by taking year 1850 as a reference. The yellow bars show the $\Delta C_{v\ dep}$ calculated based on the forest cover map in 1850, and the blue bars show the $\Delta C_{v\ dep}$ calculated based on the forest cover map for 1850 and 2010 respectively. In all cases, $\Delta C_{v\ dep}$ is estimated using the central values of parameters. Relative difference as a percentage by accounting for the forest cover change is given over each bar.

There are three reasons for the difference. First, the global total forest area had declined by 12% from 29.5 $\times 10^6$ km^2 in 1850 to 25.9 $\times 10^6$ km^2 in 2010. Second, the C response to N or P deposition varies across the five types of forest and change in the relative cover of each forest type influences the estimation of $\Delta C_{v\ dep}$. For example, the C response to N deposition is the highest for the evergreen needle-leaf forests (47 kg C kg N^{-1}) and the lowest for the evergreen broadleaf forests (12 kg C kg N^{-1}). From 1850 to 2010, the cover fraction of evergreen needle-leaf forests had increased from 19% to 21%, while the cover of evergreen broadleaf forests had decreased from 49% to 44%, leading to less reduction in $\Delta C_{N\ dep}$ than N deposition fluxes after accounting for the land cover change (Figure 9). At last, change in the spatial distribution of forests also leads to some changes in the average N or P deposition rates, but our data sets show that this influence is relatively small. The average N and P deposition rates over global forests in 2010 were 628 mg

574 N m^{-2} yr^{-1} and 47 mg P m^{-2} yr^{-1} using the forest cover map in 2010, compared with 626 mg N m^{-2} yr^{-1} and
575 49 mg P m^{-2} yr^{-1} using the forest cover map in 1850.

576

577 **4. Discussion**

578 **4.1. Global data sets of N and P deposition**

579 Our study provides the first global gridded data sets for both N and P deposition from pre-industrial (1850),
580 historical periods (1960, 1970, 1980 and 1990), to present (1997-2013), and into the future (2030, 2050 and
581 2100) from a global climate-chemistry model driven by complete bottom-up emission inventories. **Table**
582 **S1** provides a comparison of species represented by the model, horizontal resolution, and observational
583 data used to evaluate the model with previous studies. In the simulation of N, we employed state-of-the-art
584 inventories for reactive N and other tracers that influence the atmospheric chemistry of N (Klimont *et al.*,
585 2013). The chemistry of N in the model is advanced in the treatments of the ammonia cycle and the nitrate
586 particle formation (Hauglustaine *et al.*, 2014), which are only represented in few global models (Dentener
587 *et al.*, 2006). Our model also provides a horizontal resolution of 1.2°×2.5° that is finer than most of
588 previous models (Dentener *et al.*, 2006). For P, we used a new emission inventory from combustion
589 sources with the uncertainties quantified (Wang *et al.*, 2015a), which reduced the underestimation in the
590 modeled P deposition by covering P in all sizes of particles which are carried to the measurement sites.
591 Prior to our work, there was only one global data set of present day P deposition available (Mahowald *et al.*,
592 2008). In addition to its lack of temporal changes, this previous data set covered P in particles with
593 diameter smaller than 10 μm. Wang *et al.* (2015a) showed that it led to a discrepancy between the modeled
594 and observed P deposition rates at globally distributed measurement stations if P in particles with diameter
595 larger than 10 μm was neglected even if uncertainties in P emissions from other sources were accounted
596 for.

597 The modeled NO_3 and NH_4 wet deposition rates were evaluated by comparing with 8023 observations from
598 globally distributed measurement stations. The modeled P deposition rates were compared with 116
599 observations. The normalized mean bias (NMB) is -8% for the NO_3 and NH_4 wet deposition rates, and -53%
600 for the P deposition rates. It also shows that 50% of the data were associated with a bias between -25% and
601 50% for the NO_3 and NH_4 wet deposition and between -4% and 164% for the P deposition. The correlation
602 coefficient of the log-transformed deposition rate is higher for N (R=0.74) than for P (R=0.50). The
603 underestimation of P deposition was likely due to errors in the transport model or ignored local biogenic
604 aerosols in the measurement samples. The distributions of these model errors were treated as uncertainties
605 in our data sets. It is not a surprise that there is a larger uncertainty associated with the modeled deposition
606 rates of P than N. For P, in addition to the errors associated with atmospheric transport and removal,
607 emissions of P from wind erosion of soil dusts, biogenic aerosols, marine sea-salt particles, volcanoes and
608 other sources (*e.g.*, phosphine from freshwater wetlands and rice paddies) are all subject to high
609 uncertainties (Graham and Duce, 1979; Mahowald *et al.*, 2008; Wang *et al.*, 2015a). A limitation of our P
610 deposition simulations set is that the long-term variations of these emissions are not resolved, because no

information on evolution of these sources is currently available at the global scale. More measurements of P deposition rates in contrasting environments are useful to reduce the uncertainty in the modeled P deposition rates (*e.g.*, Du *et al.*, 2016), while more long-term measurements of the surface concentrations of P with additional source information are useful to constrain the model and emissions of P from difference sources (Mahowald *et al.*, 2008).

For N, we had lower model biases in some regions when compared with previous studies. For example, Hauglustaine *et al.* (2014) simulated N deposition using the same climate-chemistry model and evaluated the model using 4036 observations from global monitoring stations. They reported that NMB is respectively -32%, -4.5% and -60% in North America, Europe and Asia for the modeled NH_4 wet deposition, and -28%, 13% and -54% for the modeled NO_3 wet deposition. In contrast, NMB in our study is -12% in North America, -42% in Europe and -28% in East Asia respectively for NH_4 wet deposition, and 29%, -29% and -11% respectively for NO_3 wet deposition (**Figure S3**). Thus, our results are better for Asia but worse for Europe. Hauglustaine *et al.* (2014) attributed the underestimation in Asia to a coarse horizontal resolution of the model and an underestimation of reactive-N emissions in the region (Lamarque *et al.*, 2010). We updated reactive-N emissions by using a more recent ECLIPSE GAINS.4a inventory (Klimont *et al.*, 2013) and used a higher horizontal resolution version of the atmospheric model, from 1.9°×3.75° previously to 1.2°×2.5°. These together reduced the model bias in Asia. Despite a larger NMB in Europe in our model, the correlation coefficient (R) is 0.63 and 0.79 for wet NH_4 and NO_3 deposition in this region, respectively, higher than 0.33 and 0.49 by Hauglustaine *et al.* (2014), indicating that our model better captures the spatial pattern of N deposition.

Overall, our study provides consistent gridded simulations of both N and P deposition at a high horizontal resolution, which agrees better with observations from a large number of globally distributed measurement stations than previous studies (Mahowald *et al.*, 2008; Hauglustaine *et al.*, 2014). A statistical analysis of the model-observation comparison generates a probabilistic distribution of the model bias, which enabled us to address the uncertainty in our data sets. Whereas previous studies (de Vries *et al.*, 2014) have only estimated the C sequestration by current N deposition without spatial and temporal variations, we estimated C sink changes from changes in N and P deposition maps and included an uncertainty analysis to both N, P deposition and C sink responses.

4.2. P deposition contributes significantly to forest C storage

Increasing atmospheric CO_2 concentrations, longer growing season and N fertilization have been suggested to lead to limitation by P of productivity in temperate forests (Vitousek *et al.*, 1984, 2010; Penuelas *et al.*, 2012, 2013). Our long-term data of P-deposition rates, combined with data of N-deposition rates, suggested that $\Delta C_{P\ dep}$ would be close to $\Delta C_{N\ dep}$ if 20% of the P is fixed by soil, and C fixation due to P deposition is higher than previously estimated (Cleveland *et al.*, 2013; de Vries *et al.*, 2014) due to higher P deposition rates and a less fraction of P loss (Sattari *et al.*, 2012). Our simple stoichiometric mass balance approach indicated that the strength of P fixation by soil particles exerted the strongest influence on the response of C fixation to P deposition. Consequently, we adopted a global-constant fraction of deposited P being fixed by

soil ranging from 20% to 94%, based on the transfer coefficients between stable and labile P from Sattari *et al.* (2012). However, it should be noted that this fraction was not uniform in space and was probably soil type dependent (Compton and Cole, 1998). More field experiments measuring fixation of P by soil particles are needed to reduce this uncertainty (Johnson *et al.*, 2003).

Nevertheless, our stoichiometric method found that $\Delta C_{P\ dep}$ was equivalent to 50-90% of $\Delta C_{N\ dep}$ when the fixation of P by soil was weak, implying that deposited P can contribute to forest C storage providing that other sources of N and P were held constant. Spatially, $\Delta C_{P\ dep}$ could even exceed $\Delta C_{N\ dep}$ in some areas of forests in East Asia, South and Southeast Asia, Africa and South America (Figure 7). In particular, we find that $\Delta C_{P\ dep}$ can be significantly higher than $\Delta C_{N\ dep}$ in tropical forests in the Congo and Amazon Basins and Indonesia, due to both rapid losses of N from ecosystems through denitrification (Bai *et al.*, 2012) and high deposition rates of P from deforestation fire emissions (Giglio *et al.*, 2013). The C sink in tropical forests is sensitive to additional P inputs, because P availability in the soil of tropical forests was found to be far lower than the global average (Yang *et al.*, 2013) but P use efficiency was higher than that in boreal forests (Gill and Finzi, 2016). We suggest that more attentions should be paid to estimate the C sink due to additional P inputs from deposition in tropical forests.

However, our current knowledge of nutrient cycling is more limited for P than for N, leading to high uncertainties global ecosystem-level models (Wang *et al.*, 2010; Goll *et al.*, 2012; Yang *et al.*, 2014). It is known that most of P is neither directly taken up by plant nor lost by leaching, but a large fraction of P is fixed by soils before being slowly transferred into a labile pool that can be used by plant (Aerts and Chapin, 2000; Sattari *et al.*, 2012). Different from N, there is no atmospheric loss pathway for P, while P is less mobile in soil and hence less prone to leaching than for N (Aerts and Chapin, 2000; Goll *et al.*, 2012; Goll, 2016), but it remains unknown whether and how fast the fixed P in soil can be mineralized and used by plants (Lü *et al.*, 2013). A meta-analysis of P and N plus P fertilization experiments suggested that increasing N availability, *e.g.* from increasing N deposition, tends to increase P cycling rate and thus contributes to use of P by plants (Marklein and Houlton, 2012). Measurements of the rate of P uptake in the seasons with both high N and P-deposition rates are useful to understand the contribution of N and P deposition together to the C fixation in forests.

The cycles of C, N and P differ in their respect to the residence time in terrestrial ecosystem (Walker and Syres, 1976). Our stoichiometric method attributes the C storage due to N and P deposition at a timescale of 10-20 years, following de Vries *et al.* (2014). Nonetheless, P would turn over much more slowly than N (Walker and Syres, 1976), so it is worth highlighting that the effects of P would last longer than those of N. We expect that the use by plants is much slower for deposited P than deposited N due to the strong physical fixation of P in soil (Aerts and Chapin, 2000; Goodale *et al.*, 2002), and our estimated $\Delta C_{P\ dep}$ under a weak fixation should include part of the long-term effects of P deposition. Under a high CO_2 concentration in the near term, plants are likely increasing their efficiency in accessing and utilizing these not readily available P (Buendia *et al.*, 2014, Goll, 2016). Such effects should be better represented in the process-based models when studying the impact of N and P deposition on P limitation (Cleveland *et al.*, 2013; Wieder *et al.*,

2015).

While we cannot quantify all sources of N and P for plants, calculation of maximum and minimum $\Delta C_{v\ dep}$ by N and P provides a preliminary estimation of the C storage supported by anthropogenic P deposition. Under a weak fixation for P by soil, maximum $\Delta C_{v\ dep}$ by N and P (0.38 Pg C yr^{-1}) is 43% higher than $\Delta C_{v\ dep}$ by N alone (0.27 Pg C yr^{-1}). Meanwhile, minimum $\Delta C_{v\ dep}$ by N and P (0.10 Pg C yr^{-1}) is 53% lower than $\Delta C_{v\ dep}$ by P alone (0.22 Pg C yr^{-1}). They both suggest a potential contribution of anthropogenic P deposition to additional forest C sink. The map of $\Delta C_{v\ dep}$ by N and P also implies that other sources of N are needed to support the C storage by P deposition in some Asian tropical forests where the deposition rate increased faster for P than for N (Figure 7). However, it should be noted that N fertilization can also exert a significant effect on the capacity of plant to use the P (Marklein and Houlton, 2012; Lü *et al.*, 2013), and the maximal co-fertilized $\Delta C_{v\ dep}$ is likely even larger than maximum $\Delta C_{v\ dep}$ estimated by our method.

4.3. Uncertainty due to N retention by the canopy

We aimed at providing a preliminary estimation of forest C response to N and P deposition and investigated the imbalance of N and P in the deposition at a mid-term scale of 10-20 years when other sources were held constant. We find that anthropogenic P deposition can contribute to C storage, supplementing $\Delta C_{v\ dep}$ supported by anthropogenic N deposition by 43%. It is worth highlighting that the impact of N deposition on C storage also remains uncertain, despite more measurements of N than P retention in ecosystems, due largely to the uncertain impact of canopy N uptake. It was noticed that ~40% of N deposited is retained by the canopy in Europe and North America (Lovett and Lindberg, 1993), but the impact on C storage is not well constrained (Sparks, 2009). Sievering *et al.* (2007) found that 80% of the growing-season N deposition was retained in canopy foliage and branches and that ~20% of daytime net ecosystem exchange may be attributed to canopy N uptake. Dezi *et al.* (2010) found that the net ecosystem production would be increased by 58% under a hypothesis that canopy N uptake can directly stimulate photosynthesis relative to without canopy N uptake. Nair *et al.* (2016) suggested that accounting for canopy N uptake could lead to an increased C response to N deposition ($\Delta C/\Delta N$) from 43 to 114 kg C kg N^{-1} (by 2.6-fold) through a well-designed mesocosm experiment. It should be noted that the experiment by Nair *et al.* studied the response to N deposition at a time scale of one year and it is likely that N in the aboveground biomass can be re-allocated in plants at a longer time scale. This is likely the reason why most of applied N was retained in the plants at mid-long term (Gaige *et al.*, 2007), but most of the N in the plant was recovered in the bark rather than in the canopy (Dail *et al.*, 2009).

Here we calculated the C response to N deposition based on the fate of deposited N at a timescale of 10-20 years following de Vries *et al.* (2014). We estimated that $\Delta C/\Delta N$ was 24 kg C kg N^{-1}, which is lower than the estimate by Nair *et al.* (2016), but close to the estimate (11.5-39.8 kg C kg N^{-1}) by de Vries *et al.* (2014), because Nair *et al.* (2016) did not account for loss of N in the ecosystem via denitrification and leaching. We increased our estimate of $\Delta C_{N\ dep}$ by 2.6-fold as indicated by Nair *et al.*'s experiment to yield an upper estimate of the effect by N. Consequently, maximum $\Delta C_{v\ dep}$ by N and P increased by 2-fold from 0.38 Pg C yr^{-1} to 0.76 Pg C yr^{-1}, compared to 0.70 Pg C yr^{-1} by anthropogenic N deposition, while minimum $\Delta C_{v\ dep}$

increased by 1.6-fold from 0.10 to 0.16 Pg C yr^{-1}, compared to 0.22 Pg C yr^{-1} by anthropogenic P deposition. This suggests that the effect of P will be less significant if the high C response to N deposition due to direct use of N by the canopy can be confirmed by more evidences.

4.4. Ecological implications of N and P deposition

The spatial patterns and temporal trends of N and P emissions and subsequent deposition are important for understanding the variation of nutrient limitation in forests far away from agricultural activities (Reay *et al.*, 2008). Manipulation experiments across global biomes found that many ecosystems are co-limited by the availability of N and P (Elser *et al.*, 2007; LeBauer and Treseder, 2008; Penuelas *et al.*, 2013). Fossil fuel, biofuel and deforestation fires provide additional N and P to forests beyond the background level and these emitted from the populated regions can reach remote forests by atmospheric transport. Our long-term data of the deposition for both N and P help to quantify the deposition of N and P as anthropogenic components and to estimate the additional C storage in forests.

Global change in N and P deposition rates arising from N and P emissions by human activities and biomass burning is only one of factors that influence carbon storage by forests. Our study made a preliminary attempt to assess the contributions of forest cover change (Peng *et al.*, 2017) and the changes in N and P deposition rates to the $\Delta C_{v\ dep}$. It is not a surprise that forest cover change has offset 10% and 30% of increase in the $\Delta C_{v\ dep}$ from 1850 to 2010 due to increase in N and P deposition rates, due to decline in forest areas mainly in the tropics. In addition to forest cover change, other environmental drivers perturbing the forest C sequestration from nutrient deposition, such as rising CO_2 levels (Field *et al.*, 1995), emergency of large-scale drought (Phillips *et al.*, 2009), spring and autumn warming (Piao *et al.*, 2008) and change in forest water-use efficiency (Keenan *et al.*, 2013), are not considered in this study. A combination of our global N and P deposition data sets associated with their uncertainties with process-based vegetation models including both N and P interactions with terrestrial C cycling (*e.g.*, Wang *et al.*, 2010; Goll *et al.*, 2012) would permit a more comprehensive understanding of the impact of atmospheric deposition on the forest carbon sink.

Using a conceptual stoichiometric mass balance approach, we showed that anthropogenic N deposition for 1997-2013 contributed ~9% to the global terrestrial C sink, which is close to a previous estimate of 10% for 2030 (Reay *et al.*, 2008). We emphasized that physical P fixation is an important factor that can lead to an imbalance between N and P in atmospheric deposition. Anthropogenic P deposition (0.50 Tg P yr^{-1}) was 23-fold lower than N deposition (11.5 Tg N yr^{-1}) for 1997-2013, but most of the P was stored in soils on a shorter term and less P than N was prone to loss (5.3 Tg N yr^{-1} was lost for N by denitrification or leaching, and only 0.010 Tg P yr^{-1} was lost for P by leaching). Our analysis suggested that historical P deposition would likely exert a significant cumulative effect on the terrestrial C sink by releasing soil-fixed P in the long term. Nonetheless, our stoichiometric approach cannot account for the effects of N and P deposition under elevated CO_2 concentration and varying climate (Gruber and Galloway, 2008; Vitousek *et al.*, 2010). Comprehensive process-based Earth System ecosystem models representing the biogeochemical cycles of C, N and P are useful for understanding the ecological effects of historical, present and future depositions

of N and P on the C cycle (Reed *et al*, 2015).

Acknowledgements

The authors thank Ether/ECCAD for the distribution of emissions used in this study. This study was funded by FABIO, a Marie Curie International Incoming Fellowship funded by the European Commission (Project No 628735) and the IMBALANCE-P project of the European Research Council (ERC-2013-SyG-610028). The simulations were performed using DSM-CCRT resources under the GENCI (Grand Equipement National de Calcul Intensif) allocation of computer time (grant 2016-t2014012201).

References

Ahlström, A., Schurgers, G., Arneth, A., & Smith, B. (2012). Robustness and uncertainty in terrestrial ecosystem carbon response to CMIP5 climate change projections. *Environmental Research Letters*, **7**, 044008.

Aerts, R., & Chapin, F. S. (2000). The mineral nutrition of wild plants revisited: a re-evaluation of processes and patterns. *Advances in Ecological Research*, **30**, 1-67

Bai, E., Houlton, B. Z., & Wang, Y. P. (2012). Isotopic identification of nitrogen hotspots across natural terrestrial ecosystems. *Biogeosciences*, **9**, 3287-3304.

Balkanski, Y. (2011). L'Influence des Aérosols sur le Climat, Thèse d'Habilitation à Diriger des Recherches, Université de Versailles Saint-Quentin, Saint-Quentin-en-Yvelines.

Bouwman, A. F., Lee, D. S., Asman, W. A., Dentener, F. J., Van Der Hoek, K. W., & Olivier, J. G. J. (1997). A global high□resolution emission inventory for ammonia. *Global Biogeochemical Cycles*, **11**, 561-587.

Buendía, C., Arens, S., Hickler, T., Higgins, S. I., Porada, P., & Kleidon, A. (2014). On the potential vegetation feedbacks that enhance phosphorus availability-insights from a process-based model linking geological and ecological timescales. *Biogeosciences*, **11**, 3661-3683.

Chen, Y., Randerson, J. T., van der Werf, G. R., Morton, D. C., Mu, M. Q., & Kasibhatla, P. S. (2010). Nitrogen deposition in tropical forests from savanna and deforestation fires. *Global Change Biology*, **16**, 2024-2038.

Cleveland, C. C., Houlton, B. Z., Smith, W. K., Marklein, A. R., Reed, S. C., Parton, W., …, Running, S. W. (2013). Patterns of new versus recycled primary production in the terrestrial biosphere. *Proceedings of the National Academy of Sciences*, **110**, 12733-12737.

Compton, J. E., & Cole, D. W. (1998). Phosphorus cycling and soil P fractions in Douglas-fir and red alder stands. *Forest Ecology and Management*, **110**, 101-112.

Dail, D. B., Hollinger, D. Y., Davidson, E. A., Fernandez, I., Sievering, H. C., Scott, N. A., & Gaige, E. (2009). Distribution of nitrogen-15 tracers applied to the canopy of a mature spruce-hemlock stand, Howland, Maine, USA. *Oecologia*, 160(3): 589-599.

de Vries, W., van der Salm, C., Reinds, G. J., & Erisman, J. W. (2007). Element fluxes through European forest ecosystems and their relationships with stand and site characteristics. *Environmental Pollution*, 148, 501-513.

de Vries, W., Du, E., & Butterbach-Bahl, K. (2014). Short and long-term impacts of nitrogen deposition on

797 carbon sequestration by forest ecosystems. *Current Opinion in Environmental Sustainability*, **9**, 90-104.
798 Dentener, F., Drevet, J., Lamarque, J. F., Eickhout, B., Fiore, A. M., Hauglustaine, D., …, Wild, O. (2006).
799 Nitrogen and Sulphur Deposition on regional and global scales: a multi-model evaluation. *Global*
800 *Biogeochemical Cycles*, **20**, GB4003.
801 Dezi, S., Medlyn, B. E., Tonon, G., & Magnani, F. (2010). The effect of nitrogen deposition on forest
802 carbon sequestration: a model‐based analysis. *Global Change Biology*, **16**, 1470-1486.
803 Du, E., de Vries, W., Han, W., Liu, X. J., Yan, Z. B., & Jiang, Y. (2016). Imbalanced phosphorus and
804 nitrogen deposition in China's forests. *Atmospheric Chemistry and Physics*, **16**, 8571-8579.
805 Elser, J. J., Bracken, M. E. S., Cleland, E. E., Gruner, D. S., Harpole, W. S., Hillebrand, H., …, Smith, J. E.
806 (2007). Global analysis of nitrogen and phosphorus limitation of primary producers in freshwater, marine
807 and terrestrial ecosystems. *Ecology Letters*, **10**, 1135-1142.
808 Field, C. B., Jackson, R. B., & Mooney, H. A. (1995). Stomatal responses to increased CO_2: implications
809 from the plant to the global scale. *Plant, Cell & Environment* **18**, 1214-1225.
810 Fernández-Martinez, M., Vicca, S., Janssens, I. A., Sardans, J., Luyssaert, S., Campioli, M., …, Penuelas, J.
811 (2014). Nutrient availability as the key regulator of global forest carbon balance. *Nature Climate Change*, **4**,
812 471-476.
813 Foley, J. A., DeFries, R., Asner, G. P., Barford, C., Bonan, G., & Carpen, S. R. (2005). Global
814 consequences of land use. *Science*, **309**, 570-574.
815 Gaige, E., Dail, D. B., Hollinger, D. Y., Davidson, E. A., Fernandez, I. J., Sievering, H., …, Halteman W.
816 (2007). Changes in canopy processes following whole-forest canopy nitrogen fertilization of a mature
817 spruce-hemlock forest. *Ecosystems*, **10**, 1133-1147.
818 Galloway, J. N., Dentener, F. J., Capone, D. G., Boyer, E. W., Howarth, R. W., Seitzinger, S. P., …,
819 Voosmarty, C. J. (2004). Nitrogen cycles: past, present, and future. *Biogeochemistry*, 70, 153-226.
820 Giglio, L., Randerson, J. T., & van der Werf, G. R. (2013). Analysis of daily, monthly, and annual burned
821 area using the fourth‐generation global fire emissions database (GFED4). *Journal of Geophysical*
822 *Research: Biogeosciences*, 118, 317-328.
823 Gill, A. L., & Finzi, A. C. (2016). Belowground carbon flux links biogeochemical cycles and resource‐use
824 efficiency at the global scale. *Ecology Letters*, **19**, 1419-1428.
825 Goll, D. S., Brovkin, V., Parida, B. R., Reick, C. H., Kattge, J., Reich, P. B., …, Niinemets, U. (2012).
826 Nutrient limitation reduces land carbon uptake in simulations with a model of combined carbon, nitrogen
827 and phosphorus cycling. *Biogeosciences*, **9**, 3547-3569.
828 Goll, D. S. (2016) Coupled Cycling of Carbon, Nitrogen, and Phosphorus. In Soil Phosphorus (edited by
829 Lal Rattan Stewart, B. A.) Taylor & Francis Group, 6000 Broken Sound Parkway NW, Suite 300, Boca
830 Raton, FL 33487-2742 CRC Press.
831 Goodale, C. L., Lajtha, K., Nadelhoffer, K. J., Boyer, E. W., & Jaworski, N. A. (2002). Forest nitrogen
832 sinks in large eastern US watersheds: estimates from forest inventory and an ecosystem model. In *The*
833 *Nitrogen Cycle at Regional to Global Scales* (pp. 239-266). Springer Netherlands.

834 Goulden, M. L., McMillan, A. M. S., Winston, G. C., Rocha, A. V., Manies, K. L., Harden, J. W., &
835 Bond-Lamberty, B. P. (2011). Patterns of NPP, GPP, respiration, and NEP during boreal forest succession.
836 *Global Change Biology*, **17**, 855-871.
837 Graham, W. F., Duce, R. A. (1979). Atmospheric pathways of the phosphorus cycle. *Geochimica et*
838 *Cosmochimica Acta*, **43**, 1195-1208.
839 Granier, C., Bessagnet, B., Bond, T., D'AngiolaHugo, A., van der Gon, D., Frost, G. J., …, Liousse, C.
840 (2011). Evolution of anthropogenic and biomass burning emissions of air pollutants at global and regional
841 scales during the 1980-2010 period. *Climatic Change*, **109**, 163.
842 Gruber, N., & Galloway, J. N. (2008). An Earth-system perspective of the global nitrogen
843 cycle. *Nature*, **451**, 293-296.
844 Hansen, M. C., DeFries, R. S., Townshend, J. R., & Sohlberg, R. (2000). Global land cover classification at
845 1 km spatial resolution using a classification tree approach. *International Journal of Remote Sensing*, **21**,
846 1331-1364.
847 Hansen, M. C., Potapov, P. V., Moore, R., Hancher, M., Turubanova, S. A., Tyukavina, A., …, Townshend,
848 J. R. G. (2013). High-resolution global maps of 21st-century forest cover change. *Science*, **342**, 850-853.
849 Hauglustaine, D. A., Balkanski, Y., & Schulz, M. (2014). A global model simulation of present and future
850 nitrate aerosols and their direct radiative forcing of climate. *Atmospheric Chemistry and Physics*, **14**,
851 11031-11063.
852 Hietz, P., Turner, B. L., Wanek, W., Richter, A., Nock, C. A., & Wright, S. J. (2011). Long-term change in
853 the nitrogen cycle of tropical forests. *Science*, **334**, 664-666.
854 Holland, E. A., Braswell, B. H., Lamarque, J. F., Townsend, A., Sulzman, J. Müller, J. F., …, Roelofs, G. J.
855 (1997). Variations in the predicted spatial distribution of atmospheric nitrogen deposition and their impact
856 on carbon uptake by terrestrial ecosystems. *Journal of Geophysical Research: Atmospheres*, **102**,
857 15849-15866.
858 Houghton, R. A. (2003). Revised estimates of the annual net flux of carbon to the atmosphere from changes
859 in land use and land management 1850-2000. *Tellus B*, **55**, 378-390.
860 Hourdin, F., Musat, I., Bony, S., Braconnot, P., Codron, F., Dufresne, J. L., …, Lott, F. (2006). The
861 LMDZ4 general circulation model: climate performance and sensitivity to parametrized physics with
862 emphasis on tropical convection. *Climate Dynamics*, **27**, 787-813.
863 Hungate, B. A., Stiling, P. D., Dijkstra, P., Johnson, D. W., Ketterer, M. E., Hymus, G. J., …, Drake, B. G.
864 (2004). CO_2 elicits long-term decline in nitrogen fixation. *Science*, **304**, 1291-1291.
865 International Energy Agency (IEA). (2013). World Energy Statistics and Balances. Avaiable at:
866 http://www.oecd-ilibrary.org/statistics (accessed August 22, 2013).
867 Iversen, C. M., McCormack, M. L., Powell, A. S., Blackwood, C. B., Freschet, G. T., Kattge, J., …, Violle,
868 C. (2017). A global Fine-Root Ecology Database to address below-ground challenges in plant ecology. *New*
869 *Phytologist*, doi: 10.1111/nph.14486.
870 Johnson, A. H., Frizano, J., & Vann, D. R. (2003). Biogeochemical implications of labile phosphorus in
871 forest soils determined by the Hedley fractionation procedure. *Oecologia*, **135**, 487-499.

872 Keenan, T. F., Hollinger, D. Y., Bohrer, G., Dragoni, D., Munger, J. W., Schmid, H. P., & Richardson, A.
873 D. (2013). Increase in forest water-use efficiency as atmospheric carbon dioxide concentrations rise. *Nature*,
874 **499**, 324-327.
875 Klimont, Z., Smith, S. J., & Cofala, J. (2013). The last decade of global anthropogenic sulfur dioxide:
876 2000-2011 emissions. *Environmental Research Letter*, **8**, 014003.
877 Lamarque, J. F., Kiehl, J.T., Brasseur, G.P., Butler, T., Cameron-Smith, P, Collins, W.D., …, Thornton, P.
878 (2005). Assessing future nitrogen deposition and carbon cycle feedback using a multimodel approach:
879 Analysis of nitrogen deposition. *Journal of Geophysical Research: Atmospheres*, **110**, D19303.
880 Lamarque, J. F., Bond, T. C., Eyring, V., Granier, C., Heil, A., Klimont, Z., …, van Vuuren, D. P. (2010).
881 Historical (1850-2000) gridded anthropogenic and biomass burning emissions of reactive gases and
882 aerosols: methodology and application. *Atmospheric Chemistry and Physics*, **10**, 7017-7039.
883 Lamarque, J. F., Kyle, G. P., Meinshausen, M., Riahi, K., Smith, S. J., van Vuuren, D. P., …, Vitt, F.
884 (2011). Global and regional evolution of short-lived radiatively-active gases and aerosols in the
885 Representative Concentration Pathways. *Climatic Change*, **109**, 191.
886 Lamarque, J. F., Dentener, F., McConnell, J., Ro, C. U., Shaw, M., Vet, R., …, Nolan, M. (2013).
887 Multi-model mean nitrogen and sulfur deposition from the Atmospheric Chemistry and Climate Model
888 Intercomparison Project (ACCMIP): evaluation historical and projected changes. *Atmospheric Chemistry*
889 *and Physics*, **13**, 7997-8018.
890 Lathiere, J., Hauglustaine, D. A., Friend, A. D., Noblet-Ducoudré, N. D., Viovy, N., & Folberth, G. A.
891 (2006). Impact of climate variability and land use changes on global biogenic volatile organic compound
892 emissions. *Atmospheric Chemistry and Physics*, **6**, 2129-2146.
893 Le Quéré, C., Andrew, R. M., Canadell, J. G., Sitch, S., Korsbakken, J. I., Peters, G. P., …, Zaehle, S.
894 (2016). Global carbon budget 2016. *Earth System Science Data*, **8**, 605.
895 LeBauer, D. S., & Treseder, K. K. (2008). Nitrogen limitation of net primary productivity in terrestrial
896 ecosystems is globally distributed. *Ecology*, **89**, 371-379.
897 Liu, L., & Greaver, T. L. (2009). A review of nitrogen enrichment effects on three biogenic GHGs: the CO_2
898 sink may be largely offset by stimulated N_2O and CH_4 emission. *Ecology Letters*, **12**, 1103-1117.
899 Lovett, G. M., & Lindberg, S. E. (1993). Atmospheric deposition and canopy interactions of nitrogen in
900 forests. *Canadian Journal of Forest Research*, **23**, 1603-1616.
901 Lü, X. T., Reed, S., Yu, Q., He, N. P., Wang, Z. W., Han, X. G. (2013). Convergent responses of nitrogen
902 and phosphorus resorption to nitrogen inputs in a semiarid grassland. *Global Change Biology*, **19**,
903 2775-2784.
904 Magnani, F., Mencuccini, M., Borghetti, M., Berbigier, P., Berninger, F., Delzon, S., …, Grace, J. (2007).
905 The human footprint in the carbon cycle of temperate and boreal forests. *Nature*, **447**, 849-851.
906 Mahowald, N., Jickells, T. D., Baker, A. R., Artaxo, P., Benitez-Nelson, C. R., Bergametti, G., …, Tsukuda,
907 S. (2008). Global distribution of atmospheric phosphorus sources, concentrations and deposition rates, and
908 anthropogenic impacts. *Global Biogeochemical Cycles*, **22**, GB4026.
909 Mahowald, N. (2011). Aerosol indirect effect on biogeochemical cycles and climate. *Science*, **334**,

794-796.

Marklein, A. R., & Houlton, B. Z. (2012). Nitrogen inputs accelerate phosphorus cycling rates across a wide variety of terrestrial ecosystems. *New Phytologist*, **193**, 696-704.

Matthews, H. D. (2007). Implications of CO_2 fertilization for future climate change in a coupled climate-carbon model. *Global Change Biology*, **13**, 1068-1078.

Nadelhoffer KJ, Emmett BA, Gundersen P, Kjønaas, O. J., Koopmans, C. J., Schleppi, P., …, Wright, R. F. (1999). Nitrogen deposition makes a minor contribution to carbon sequestration in temperate forests. *Nature*, **398**, 145-148.

Nair, R. K., Perks, M. P., Weatherall, A., Baggs, E. M., & Mencuccini, M. (2016). Does canopy nitrogen uptake enhance carbon sequestration by trees? *Global change biology*, **22**, 875-888.

Norby, R. J., Warren, J. M., Iversen, C. M., Medlyn, B. E., & McMurtrie, R. E. (2010). CO_2 enhancement of forest productivity constrained by limited nitrogen availability. *Proceedings of the National Academy of Sciences*, **107**, 19368-19373.

Okin, G. S., Mahowald, N., Chadwick, O. A., & Artaxo, P. (2004). Impact of desert dust on the biogeochemistry of phosphorus in terrestrial ecosystems. *Global Biogeochemical Cycles*, **18**, GB2005.

Paulot, F., Jacob, D. J., & Henze, D. K. (2013). Sources and processes contributing to nitrogen deposition: An adjoint model analysis applied to biodiversity hotspots worldwide. *Environmental Science & Technology*, **47**, 3226-3233.

Paulot, F., Jacob, D. J., Johnson, M. T., Bell, T. G., Baker, A. R., Keene, W. C., …, Stock, C. A. (2015). Global oceanic emission of ammonia: Constraints from seawater and atmospheric observations. *Global Biogeochemical Cycles*, **29**, 1165-1178.

Peng, S., Ciais, P., Maignan, F., Li, W., Chang, J. F., Wang, T., & Yue, C. (2017). Sensitivity of land-use change emission estimates to historical land-use and land-cover mapping. *Global Biogeochemical Cycles*, 31, doi:10.1002/2015GB005360.

Peñuelas, J., Sardans, J., Rivas□Ubach, A., & Janssens, I. A. (2012). The human□induced imbalance between C, N and P in Earth's life system. *Global Change Biology*, **18**, 3-6.

Penuelas, J., Poulter, B., Sardans, J., Ciais, P., van der Velde, M., Bopp, L., …, Janssens, I. A. (2013). Human-induced nitrogen–phosphorus imbalances alter natural and managed ecosystems across the globe. *Nature Communications*, **4**, 2934.

Phillips, O. L., Aragão, L. E. O. C., Lewis, S. L., Fisher, J. B., Lloyd, J., López-González, G., …, Torres-Lezama, A. (2009). Drought sensitivity of the Amazon rainforest. *Science*, **323**, 1344-1347.

Phoenix, G. K., Hicks, W. K., Cinderby, S., Kuylenstierna, J. C. I., Stock, W. D., Dentener, F. J., …, Ineson, P. (2006). Atmospheric nitrogen deposition in world biodiversity hotspots: the need for a greater global perspective in assessing N deposition impacts. *Global Change Biology*, **12**, 470-476.

Piao, S., Ciais, P., Friedlingstein, P., Peylin, P., Reichstein, M., Luyssaert, S., …, Vesala, T. (2008). Net carbon dioxide losses of northern ecosystems in response to autumn warming. *Nature*, **451**, 49-52.

Reay, D. S., Dentener, F., Smith, P., Grace, J., & Feely, R. A. (2008). Global nitrogen deposition and carbon sinks. *Nature Geoscience*, **1**, 430-437.

948 Reed, S. C., Yang, X., & Thornton, P. E. (2015). Incorporating phosphorus cycling into global modeling
949 efforts: a worthwhile, tractable endeavor. *New Phytologist*, **208**, 324-329.
950 Reich, P. B., Hobbie, S. E., Lee, T., Ellsworth, D. S., West, J. B., Tilman, D., …, Trost, J. (2006). Nitrogen
951 limitation constrains sustainability of ecosystem response to CO_2. *Nature*, **440**, 922-925.
952 Riahi, K., Grübler, A., & Nakicenovic, N. (2007). Scenarios of long-term socio-economic and
953 environmental development under climate stabilization. *Technological Forecasting and Social Change*, **74**,
954 887-935.
955 Rowe, E. C., Smart, S. M., Kennedy, V. H., Emmett, B. A., & Evans, C. D. (2008). Nitrogen deposition
956 increases the acquisition of phosphorus and potassium by heather Calluna vulgaris. *Environmental*
957 *Pollution*, **155**, 201-207.
958 Sardans, J., & Peñuelas, J. (2013). Tree growth changes with climate and forest type are associated with
959 relative allocation of nutrients, especially phosphorus, to leaves and wood. *Global Ecology and*
960 *Biogeography*, **22**, 494-507.
961 Sardans, J., & Peñuelas, J. (2015) Potassium: a neglected nutrient in global change. *Global Ecology and*
962 *Biogeography*, **24**, 261-275.
963 Sattari, S. Z., Bouwman, A. F., Giller, K. E., & van Ittersum, M. K. (2012). Residual soil phosphorus as the
964 missing piece in the global phosphorus crisis puzzle. *Proceedings of the National Academy of Sciences*, **109**,
965 6348-6353.
966 Schlesinger, W. H. (2009). On the fate of anthropogenic nitrogen. *Proceedings of the National Academy of*
967 *Sciences*, **106**, 203-208.
968 Sievering, H., Tomaszewski, T., & Torizzo, J. (2007). Canopy uptake of atmospheric N deposition at a
969 conifer forest: part I□canopy N budget, photosynthetic efficiency and net ecosystem exchange. *Tellus B*, **59**,
970 483-492.
971 Sparks, J. P. (2009). Ecological ramifications of the direct foliar uptake of nitrogen. *Oecologia*, **159**, 1-13.
972 Templer, P. H., Mack, M. C., Chapin III, F. S., Christenson, L. M., Compton, J. E., Crook, H. D., …, Zak,
973 D. R. (2012). Sinks for nitrogen inputs in terrestrial ecosystems: a meta□analysis of 15N tracer field
974 studies. *Ecology*, **93**, 1816-1829.
975 Thomas, R. Q., Canham, C. D., Weathers, K. C., & Goodale, C. L. (2010). Increased tree carbon storage in
976 response to nitrogen deposition in the US. *Nature Geoscience*, **3**, 13-17.
977 Thornton, P. E., Doney, S. C., Lindsay, K., Moore, J. K., Mahowald, N., Randerson, J. T., …, Lee, Y. H.
978 (2009). Carbon-nitrogen interactions regulate climate-carbon cycle feedbacks: results from an
979 atmosphere-ocean general circulation model. *Biogeosciences*, **6**, 2099-2120.
980 Tipping, E., Benham, S., Boyle, J. F., Crow, P., Davies, J., Fischer, U., …, Toberman, H. (2014).
981 Atmospheric deposition of phosphorus to land and freshwater. *Environmental Science: Processes &*
982 *Impacts*, **16**, 1608-1617.
983 van der Werf, G. R., Randerson, J. T., Collatz, G. J., Giglio, L., Kasibhatla, P. S., Arellano Jr, A. F., …,
984 Kasischke, E. S. (2004). Continental-scale partitioning of fire emissions during the 1997 to 2001 El
985 Nino/La Nina period. *Science*, **303**, 73-76.

Vet, R., Artz, R. S., Carou, S., Shaw, M., Ro, C. U., Aas, W., …, Reid, N. W. (2014). A global assessment of precipitation chemistry and deposition of sulfur, nitrogen, sea salt, base cations, organic acids, acidity and pH, and phosphorus. *Atmospheric Environment*, **93**, 3-100.

Vitousek, P. M. (1984). Litterfall, nutrient cycling, and nutrient limitation in tropical forests. *Ecology*, **65**, 285-298.

Vitousek, P. M., Porder, S., Houlton, B. Z., & Chadwick, O. A. (2010). Terrestrial phosphorus limitation: mechanisms, implications, and nitrogen–phosphorus interactions. *Ecological Applications*, **20**, 5-15.

Walker, T. W., & Syers, J. K. (1976). The fate of phosphorus during pedogenesis. *Geoderma*, **15**, 1-19.

Wang, Y. P., Law, R. M., & Pak, B. (2010). A global model of carbon, nitrogen and phosphorus cycles for the terrestrial biosphere. *Biogeosciences*, **7**, 2261-2282.

Wang, R., Balkanski, Y., Boucher, O., Ciais, P., Peñuelas, J., & Tao, S. (2015a). Significant contribution of combustion-related emissions to the atmospheric phosphorus budget. *Nature Geoscience*, **8**, 48-54.

Wang, R., Balkanski, Y., Bopp, L., Aumont, O., Boucher, O., Ciais, P., …, Tao, S. (2015b). Influence of anthropogenic aerosol deposition on the relationship between oceanic productivity and warming. *Geophysical Research Letters*, **42**, 10745-10754.

Westerling, A. L., Hidalgo, H. G., Cayan, D. R., & Swetnam, T. W. (2006). Warming and earlier spring increase western US forest wildfire activity. *Science*, **313**, 940-943.

Wieder, W. R., Cleveland, C. C., Smith, W. K., & Todd-Brown, K. (2015). Future productivity and carbon storage limited by terrestrial nutrient availability. *Nature Geoscience*, **8**, 441-444.

Xu, X., Thornton, P. E., & Post, W. M. (2013). A global analysis of soil microbial biomass carbon, nitrogen and phosphorus in terrestrial ecosystems. *Global Ecology and Biogeography*, **22**, 737-749.

Yang, X., Post, W. M., Thornton, P. E., & Jain, A. (2013). The distribution of soil phosphorus for global biogeochemical modeling. *Biogeosciences*, **10**, 2525.

Yang, X., Thornton, P. E., Ricciuto, D. M., & Post, W. M. (2014). The role of phosphorus dynamics in tropical forests. *Biogeosciences*, **11**, 1667.

Zaehle, S., Friedlingstein, P., & Friend, A. D. (2010). Terrestrial nitrogen feedbacks may accelerate future climate change. *Geophysical Research Letters*, *37*, L01401.

Zaehle, S., Medlyn, B. E., De Kauwe, M. G., Walker, A. P., Dietze, M. C., Hickler, T., …, Norby, R. J. (2014). Evaluation of 11 terrestrial carbon-nitrogen cycle models against observations from two temperate Free□Air CO_2 Enrichment studies. *New Phytologist*, **202**, 803-822.

Zhu, Z., Piao, S., Myneni, R. B., Huang, M. T., Zeng, Z. Z., Canadell, J. G., …, Zeng, N. (2016). Greening of the Earth and its drivers. Nature Climate Change, **6**, 791-795.